Energy & Environmental Science

REVIEW

View Article Online
View Journal | View Issue

Cite this: *Energy Environ. Sci.*, 2016, **9**, 357

The application of graphene and its composites in oxygen reduction electrocatalysis: a perspective and review of recent progress

Drew Higgins, Pouyan Zamani, Aiping Yu and Zhongwei Chen*

The pressing necessity of a sustainable energy economy renders electrochemical energy conversion technologies, such as polymer electrolyte fuel cells or metal–air batteries, of paramount importance. The implementation of these technologies at scale still faces cost and operational durability challenges that stem from the conventionally used oxygen reduction reaction (ORR) electrocatalysts. While years of progress in ORR catalyst research has yielded some very attractive material designs, further advances are still required. Graphene entered the picture over 10 years ago, and scientists have only recently achieved a level of understanding regarding how its specific properties can be fine-tuned for electrocatalyst applications. This paper provides a critical review of the knowledge generated and progress realized over these past years for the development of graphene-based ORR catalysts. The first section discusses the application potential of graphene or modified graphene as platinum nanoparticle catalyst supports. The second section discusses the important role that graphene has played in the development of non-precious metal ORR catalysts, and more particularly its role in pyrolyzed transition metal–nitrogen–carbon complexes or as a support for inorganic nanoparticles. Finally the development of heteroatom doped graphene species is discussed, as this has been demonstrated as an excellent method to fine-tune the physicochemical properties and induce catalytic activity. Throughout this paper, clear differentiation is made between acidic and alkaline ORR catalysts, and some common misconceptions or improper testing practices used throughout the literature are revealed. Synthesis strategies and how they pertain to the resulting structure and electrochemical performance of graphene are discussed. In light of the large body of work done in this area, specific strategies are suggested for perpetuating the advancement of graphene-based ORR electrocatalysts. With concerted efforts it is one day likely that graphene-based catalysts will be a staple of electrochemical energy systems.

Received 12th August 2015,
Accepted 5th November 2015

DOI: 10.1039/c5ee02474a

www.rsc.org/ees

Broader context

Since its discovery just over 10 years ago, graphene and its derivatives have shaped the materials science landscape. The attractive properties of graphene-based materials have in particular warranted significant investigative efforts in the electrocatalysis community, as this is a field that can readily leverage the tunable surface chemistry and high surface areas. This review article provides a detailed account of recent progress in the development of graphene-based oxygen reduction catalysts. The oxygen reduction reaction is of fundamental importance to several clean operating electrochemical energy conversion and storage technologies, including polymer electrolyte fuel cells and rechargeable metal–air batteries. These devices are touted as integral components of future generation sustainable energy infrastructures, provided some of their technical challenges can be sufficiently addressed. As ORR catalysts are generally one of the most expensive components in these devices, while also serving as the performance and durability limiting factor, graphene has the potential to provide revolutionary advances in this area. This article highlights areas where fundamental knowledge is still needed and discusses avenues for continued progress. Additionally, robust testing protocols are suggested for evaluating and comparing graphene-based electrocatalyst performance.

1. Introduction

1.1. Electrochemical energy technologies (*i.e.*, fuel cells/metal–air batteries)

In the 21st century, the topic of energy has secured a foothold as one of the most important technological issues that must be

Department of Chemical Engineering, University of Waterloo, 200 University Ave. W., Waterloo, Ontario, Canada, N2L 3G1. E-mail: zhwchen@uwaterloo.ca

addressed to secure the sustainability of human societies. Global energy demands continually soar to new highs, with average growth rates in the consumption of energy soaring by over 50% in a 25 year period (from 1987 to 2012).[1] Fossil fuel resources are thereby being consumed at unprecedented rates, leading to greenhouse gas emissions of more than 31 billion tonnes of CO_2 equivalent due to the relatively "dirty" combustion process. It is clear that, as a society, we require transformative clean technologies that can revolutionize the way we produce, transport and use energy. The requirements of such technologies are no easy feat. They must be sustainable, clean operating, practically viable in terms of performance capabilities and efficiency, and most importantly, they must be affordable.

Electrochemical devices have demonstrated the capacity to satisfy all of these requirements, operating with only environmentally benign emissions and boasting excellent operational efficiencies. While the commercial success of electrochemical devices is ubiquitous, they have not had such an impact in sectors that are huge greenhouse gas emitters, such as transportation applications or utility scale power production. For example, polymer electrolyte fuel cells (PEFCs) have already found niche markets in telecommunications backup power and materials handling (*i.e.*, forklift) fleets.[2] Further development is needed however to one day realize the ideal promise of replacing the internal combustion engines in conventional automobiles (*vide infra*).[3] This would allow society to capitalize on the advantages of PEFCs, most notable being the abilities to achieve "well to wheels" greenhouse gas emissions that approach zero.[4] PEFC vehicles are particularly attractive due to their driving range that can exceed 500 km with the ability to be refuelled in 3–5 minutes. The size, weight and cost of a lithium-ion battery that could achieve this driving range would not be attractive to end users. Current battery and charging technologies also cannot provide a full recharge in this time frame.

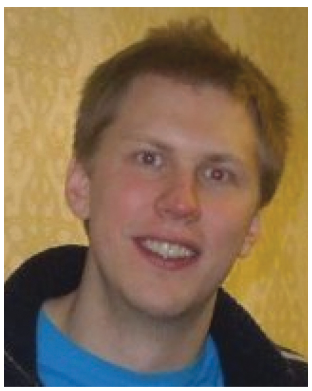

Drew Higgins

Drew Higgins obtained his PhD in Chemical Engineering from the University of Waterloo in July, 2015. His dissertation work was under the supervision of Dr Zhongwei Chen, during which time he spent nearly one year as a Visiting Scholar at the Los Alamos National Laboratory. He is now an NSERC Banting Postdoctoral Fellow at Stanford University, working under the supervision of Professor Thomas Jaramillo. His research interests include the development of nanostructured functional materials and their integration into clean energy electrochemical devices.

Pouyan Zamani

Pouyan Zamani is a PhD student in Chemical Engineering at the University of Waterloo (since 2012) under the supervision of Dr Zhongwei Chen, with a focus on the development of nano-structured metal–nitrogen–carbon based materials as non-precious oxygen reduction reaction catalysts for fuel cell applications.

Aiping Yu

Dr Aiping Yu has over 15 years of experience focusing on development, processing and functionalization of nanostructured carbon materials, along with their application as electrode materials in high performance supercapacitors. She has published over 56 refereed journal papers, mostly in high impact journals such as Science, Advanced Materials, Energy and Environment Science, and Nano Letters. She has also published two review papers, two book chapters and one book on supercapacitors. These publications have received over 5000 citations. She holds 7 patents and provisional patents for graphene nanomaterials. Two of these are licensed to companies such as Tessera, Inc., and Grafoid, Inc.

Zhongwei Chen

Dr Zhongwei Chen is Canada Research Chair in Advanced Materials for Clean Energy at the University of Waterloo. His research interests are in the development of advanced energy materials for metal–air batteries, lithium-ion batteries and fuel cells. He was promoted to an Associate Professor with early tenure in 2012 and was awarded the Canada Research Chair in 2014. He has published 1 book, 6 book chapters and more than 130 peer-reviewed journal articles with over 10 000 citations and H-index of 43 (GoogleScholar). He is listed as inventor on 15 US/international patents, with several licensed to companies in USA and Canada.

Rechargeable metal–air batteries are also attractive for transportation applications owing to their open air electrode concept that results in energy densities much higher than other battery chemistries. In addition to PEFCs and redox-flow batteries,[5–7] rechargeable metal–air batteries are also being touted as promising devices in the research and development stage for grid scale energy storage.[8,9] By scaling these technologies into large stacks, they can be coupled with clean wind and solar energy production to overcome the associated intermittency issues.

While the target markets exist and are anxiously awaiting the arrival of practically viable clean energy technologies, remaining technical challenges must be addressed for PEFCs and metal–air batteries. These challenges relate to cost and durability.[3] Cost reductions and durability improvements must be sufficiently achieved to render these electrochemical devices commercially competitive with conventional technologies, such as the internal combustion engine used in transportation applications. In PEFCs and rechargeable metal–air batteries, although several functional components work in tandem to produce electricity from the chemical energy stored in oxygen and hydrogen/metal electrodes, the majority of cost and durability issues arise from the cathode.[10–14] This is where the electrochemical oxygen reduction reaction (ORR) occurs, facilitated by catalysts that are commonly comprised of platinum or other expensive constituents. Reducing the dependency on expensive catalyst technologies can only be accomplished by developing new catalyst systems that can achieve improved activity and performance, while simultaneously providing cost reductions.

1.2. Oxygen reduction electrocatalysis

The commonality between various types of PEFCs and primary metal–air batteries is that the ORR is a fundamental backbone of their operation. Rechargeable metal–air batteries also incorporate an oxygen evolving catalyst into the electrode, a topic that is outside the scope of the current review paper. Comparing PEFCs and metal–air batteries, the biggest differentiating factor is the type of electrolyte membrane employed. Based on its nature, the electrolytes are classified into two groups, acidic or alkaline. In alkaline electrolyte membranes, hydroxide anions are transported from the cathode to the anode. These are used in metal–air batteries or alkaline exchange membrane fuel cells (which technically are also a type of PEFC). Acidic electrolyte membranes facilitate the transport of protons to the anode to the cathode, and are used in the PEFCs rigorously under investigation for automotive applications. For this reason, the term PEFC term will be reserved for these devices throughout this paper. The acidic or alkaline nature of the electrolyte membrane also directly governs the electrochemical pathways of the oxygen reducing cathode electrode as displayed in Fig. 1.

In acidic electrolytes, the ORR occurs either by the four electron reduction (eqn (1)), or the two electron reduction (eqn (2)). The overall four electron reduction mechanism is favourable owing to its obvious efficiency advantages (four electrons per oxygen molecule), and because it avoids the formation of hydrogen peroxide species in the electrode that

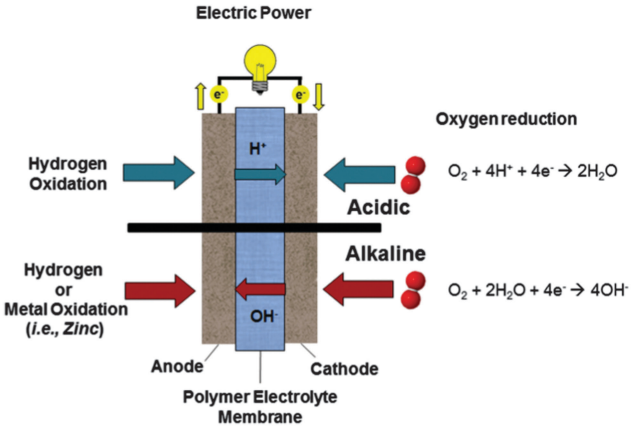

Fig. 1 Schematic of typical pathways of oxygen reduction in (top) acidic PEFCs and (bottom) alkaline operating fuel cells or metal–air batteries during discharge.

can cause membrane and ionomer degradation.[15–17] The ORR process can also occur by a two-step reduction (overall four electrons), in which hydrogen peroxide species can be directly or indirectly reduced to water.

$$O_2 + 4H^+ + 4e^- \rightarrow 2H_2O \quad (1)$$

$$O_2 + 2H^+ + 2e^- \rightarrow H_2O_2 \quad (2)$$

Under acidic conditions, such as those employed in PEFCs for transportation applications, platinum is the only catalyst that, to date, can provide suitable activity and stability. As the acidic ORR is inherently several order of magnitude slower than the anodic hydrogen oxidation,[18] rapid oxygen reduction kinetics are a necessity from a performance standpoint. Efforts are being undertaken to develop catalysts with further increased activity towards the ORR, allowing for a reduction in the content of expensive platinum required to achieve suitable power output (*i.e.*, increased electrocatalytic activity on a platinum mass basis). Graphene has recently emerged as a material of interest in this field, with some research teams developing graphene-based platinum nanoparticle supports that demonstrates improved electrochemical activity and durability compared with conventional carbon black supported platinum (traditionally referred to as Pt/C).[19–22] Graphene-based materials have also played an important role in non-platinum group metal (non-PGM) catalyst investigations.[23–27] This is the holy grail of oxygen reduction electrocatalysis research as it would allow fuel cell manufacturers to eliminate the platinum content of the cathode electrode entirely. Although non-PGM catalyst solutions may still be years off in terms of bridging the gap between current performance metrics and those of platinum, graphene has been shown to play a role in this strategic area of research and is an important avenue moving forward.

Analogous to acidic conditions, in alkaline conditions the ORR can either occur by a four electron reduction (eqn (3)) or two electron reduction forming hydrogen peroxide species (eqn (4)).

$$O_2 + 2H_2O + 4e^- \rightarrow 4OH^- \quad (3)$$

$$O_2 + H_2O + 2e^- \rightarrow HO_2^- + OH^- \quad (4)$$

The ORR kinetics are dramatically more favourable in alkaline conditions, providing opportunity to use a host of non-PGM catalysts, including silver,[28] metal-oxides[29–31] or nitrogen-doped carbon nanostructures.[32–34] While this provides ideal cost savings in comparison to precious metal alternatives, it is important that these materials provide high enough activity to facilitate the four electrons ORR with sufficiently low overpotentials. Numerous graphene and graphene-composite catalysts have been shown to provide excellent activity and stability in alkaline conditions.[35,36] It is hoped that the work ongoing in this field and reviewed within this paper creates a pathway to develop advanced high activity and low catalyst technologies.

1.3. Graphene

On the fundamental level, graphene is a monolayer two-dimensional sheet of carbon atoms chemically bonded in the hexagonal pattern that is characteristic of graphite. Marking just over a decade since its first inception in 2004,[37] graphene is attractive from both a fundamental and applied standpoint, owing to its fascinating electronic, surface and mechanical properties.[38,39] By employing different synthetic or processing methods, researchers are also able to fine-tune the intrinsic material properties of these materials. This bodes well for electrocatalysis, as the surface-specific processes and reaction rates are governed by the catalyst properties that can be modulated. Whether acting as a catalyst itself, or interacting with catalytic particles deposited on the surface, rational design of graphene allows one to ''tinker'' the electrocatalytic behaviour in a way that is favourable for achieving improved oxygen reduction kinetics.

It should be noted that there are inconsistencies throughout the literature regarding the nomenclature of graphene and related materials. A large portion of ''graphene'' reported in the literature consists of multiple stacked layers, and over time the term graphene has expanded to incorrectly encompass a broad range of derivative materials. It is clear that a unified naming convention is necessary and was the topic of an editorial published in the journal *Carbon* in 2013.[40] These authors put forth a suggested naming convention that is applied throughout this manuscript with the relevant terms summarized in Table 1. Specifically, the term ''graphene'' should be reserved for the isolated monolayer form of hexagonally arranged carbon bonded in the sp^2 configuration. ''Graphite oxide'' is a solid material prepared by oxidation of graphite to functionalize the basal planes and increase the interlayer spacing. ''Graphene oxide'' (GO) is the exfoliated form of graphite oxide and is commonly prepared by dispersing this highly soluble material in an aqueous solvent. Finally, reduced graphene oxide (rGO), as the name suggests, results from the reduction of GO. We will also encompass the many derivatives of the graphene family throughout the manuscript with the term ''graphene-based materials''.

There are several review papers dedicated to understanding the fascinating properties of graphene-based materials, while also outlining synthesis techniques and approaches used throughout the field.[24,39,41–43] The preparation of graphene-based catalysts generally involves oxidation of graphite powder by the widely utilized Hummers' method.[44] The resulting GO species are then reduced to rGO by a wide range of techniques, with the most commonly utilized being thermal,[45] chemical[46] or hydro/solvothermal[47] reduction. The appeal of these methods is that reasonable yields can be produced from readily available graphite precursors. An additional benefit is that GO has a very high surface concentration of oxygen functional species (*i.e.*, hydroxyl, carbonyl, carboxylic, and epoxy)[48] that provide reactive sites and excellent dispersion in solutions in comparison to the basal plane of graphene. These oxygen species are removed to varying extents during reduction, but also act as anchoring points for the functionalization or doping of the graphene structure. In particular, functionalization involves groups covalently bonded to the surface of graphene, whereas doping refers to the actual incorporation of heteroatoms into the carbon lattice. For example, nitrogen dopants are capable of directly replacing sp^2 bonded basal carbon in the ''graphitic-N'' arrangement, or residing on the edges of graphene in the pyridinic-N (6-membered ring), or pyrollic-N (5 membered ring).[41,49] Both functionalization and doping will modulate the properties of graphene and are capable of inducing desirable interactions with other molecules. These approaches thereby hold an important place in electrocatalysis and have led to some of the progress discussed within this review.

1.4. Scope and outline

Scientists are just beginning to understand the wide realm of capabilities that can be achieved by carefully designed and integrated graphene-based materials. The application potential towards two important electrochemical devices that rely on oxygen reduction: PEFCs and metal–air batteries, is undergoing intensive development with marked progress realized in recent years. The ability to understand and manipulate the properties of graphene and its composites may hold the key to revolutionizing the performance capabilities of these modern clean energy technologies and is the focus of the current review paper. Recent research progress towards graphene-based catalysts for the

Table 1 Nomenclature used for graphene family materials

Material	Abbreviation	Description
Graphene	—	Two dimensional sp^2 bonded carbon layer in a hexagonal arrangement with single atom thickness
Graphite oxide	—	Graphite that has been oxidized to provide oxygen functional groups on the basal planes and increase interlayer spacing
Graphene oxide	GO	Exfoliated form of graphite oxide
Reduced graphene oxide	rGO	Product of the reduction (chemical, thermal, solvothermal, *etc.*) of graphene oxide

electrochemical reduction of oxygen will be highlighted. The current state of understanding, along with the remaining technical challenges in this field of discovery will be discussed in context of the large body of work accomplished to date. Potential avenues of research will be suggested, with a focus placed on propelling the performance of graphene-based catalysts towards feasibility, and for filling voids of knowledge regarding the fundamental properties of these materials. An effort will be placed on discussing appropriate methods of ORR activity evaluation and results interpretation in an attempt to correct some of the common misconceptions and improper practices used throughout the scientific community. With this, we hope to aid in successfully translating advances made in the materials science of graphene, into practical materials solutions for electrocatalysis and electrochemical energy technologies.

This review paper will outline recent bodies of work on the application and role of graphene in oxygen reduction electrocatalysis, divided into three main chapters based on the type of graphene-based materials being developed. In Section 2, the development of graphene (both doped and undoped) supported platinum catalysts will be reviewed and discussed. Graphene-based materials can induce favourable catalyst–support interactions to provide stability and activity enhancements on a platinum-mass basis, thereby leading to reduced precious metal loadings in the acidic PEFCs under development for transportation applications. Section 3 will focus on graphene-based non-precious metal catalysts. The discussion will focus on the important role of graphene-like structures in pyrolyzed metal–nitrogen–carbon complexes or as supports for inorganic particle catalysts. Section 4 will focus on the development of heteroatom-doped graphenes for ORR electrocatalysis, with nitrogen-doped graphene-based materials the most thoroughly investigated configuration. Recent progress on dual-doping or compositing graphene-based materials with other nanostructured carbons (*i.e.*, carbon nanotubes or graphene quantum dots) will also be highlighted, as these comprise very promising strategies to achieve unprecedented catalytic performance among related materials. Throughout the paper, clear differentiation between graphene-based catalysts for acid and alkaline conditions will be made, bearing in mind that the alkaline ORR is a much more favourable process. The techniques to prepare the most promising graphene-based catalyst configurations will also be highlighted, along with specifying missing bits of fundamental knowledge that will be beneficial for future material designs.

2. Graphene as a platinum support

Ideal platinum catalyst supports boast several features including high surface areas, electronic conductivity, electrochemical stability and the ability to homogeneously distribute uniformly sized nanoparticles. Graphene has the ability to meet all of these criteria and its derivatives have emerged as promising platinum electrocatalyst supports. In this section, we will first discuss platinum catalysts supported directly on graphene-based materials, or anchored using a surface functionalization approach. We will then discuss graphene-based supports that are doped with heteroatom species (*i.e.*, nitrogen or sulfur), with the distinction from functionalized graphene lying in that these foreign heteroatom are incorporated directly into the graphitic planes.

2.1. Platinum supported on non-doped graphene

Because of the highly graphitic features of graphene that can ideally provide resistivity to carbon corrosion during fuel cell operation, the basal plane surfaces are not favourable for interaction with platinum species. This can make it difficult to deposit well-dispersed, uniform size nanoparticles, and instead commonly results in agglomerate platinum structures or nanoparticle deposition restricted to edge sites. This is analogous to the well-established properties and surface interactions of carbon nanotubes (CNTs), where functionalization procedures are commonly employed to facilitate a good dispersion of catalyst particles.[50]

Different scientists have aimed to aid and strengthen the deposition of platinum nanoparticles by using poly(diallyldimethylammonium chloride), termed PDDA, to functionalize the surface of graphene nanoplatelets[51] or GO.[52] Each of these approaches demonstrated excellent dispersivity of *ca.* 2–3 nm particles that possessed good electrochemical stability through half-cell investigations. It is well known however that platinum surfaces are prone to contamination by small adsorbing molecules, surfactants and polymers that could potentially inhibit the practicality of this approach owing to the inevitable active site blockages that will occur even with trace amounts of residual species.[17]

Recognizing this, Zeng *et al.*[53] devised a creative approach to functionalize GO with an in-house prepared anion exchange ionomer (AEI), namely quaternary ammonia poly(2,6-dimethyl-1,4-phenylene oxide). They strategically opted to use this AEI because it is the same class of ionomer that is required as an additive to the electrodes of alkaline-based fuel cells to conduct hydroxide species produced at the anode (analogous to Nafion ionomers used in PEFCs). It was shown that functionalization of GO with the AEI allowed for smaller average platinum nanoparticle sizes (*ca.* 2.46 nm) than could be obtained when AEI was not used (*ca.* 3.95 nm) during catalyst preparation (Fig. 2a). Half-cell electrochemical investigations in 0.1 M potassium hydroxide (KOH) indicated that improved activity towards the ORR could be achieved on the prepared Pt/AEI/rGO, likely related to the increased electrochemical surface area (ECSA) values that accompany reduced diameter platinum nanoparticles. Prepared catalysts were spray-coated onto an alkaline exchange membrane (AEM) and subjected to AEM fuel cell testing. The benefits of the reduced platinum size was clear, with the Pt/AEI/rGO catalyst displaying the highest performance in comparison to AEI free Pt/rGO and commercial Pt/C catalyst (Fig. 2b). It was also clear that the removal of the AEI was completely unnecessary, and in fact, further performance improvements were realized by incorporating higher contents of AEI during electrode preparation. A maximum power density of 264.8 mW cm^{-2} was achieved for the Pt/AEI/rGO based membrane electrode assembly (MEA) prepared with additional AEI (Fig. 2c). He *et al.*[54] were also able to anchor uniformly

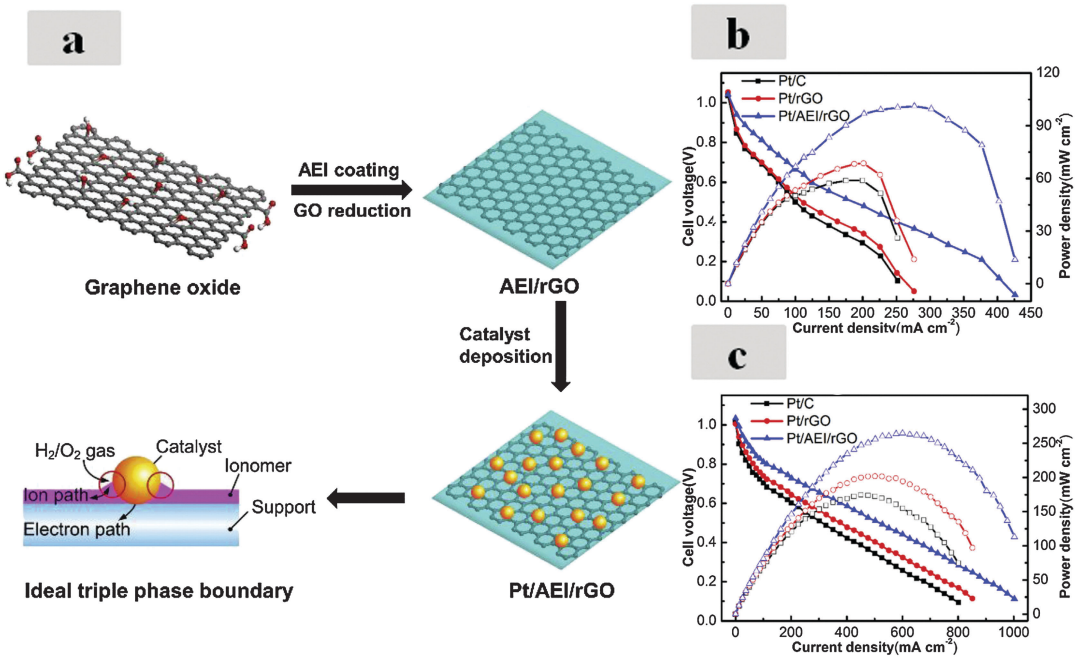

Fig. 2 (a) Schematic of Pt/AEI/rGO catalyst preparation with ideal triple phase boundary. (b) Power densities (empty symbols) and polarization (filled symbols) curves for a H_2/O_2 AEM fuel cell without additional ionomer and (c) the catalyst layers with a total of 20 wt% ionomer. Reprinted from ref. 53 copyright (2015), with permission from Elsevier.

dispersed platinum nanoparticles (1–4 nm) on rGO functionalized with perfluorosulfonic acid, the proton conducting ionomer conventionally used in acidic based PEFCs.

To achieve excellent platinum nanoparticle dispersion, other research teams have used GO during the deposition step. GO has a high concentration of surface functional species that ideally make it readily dispersed in a large number of solvents[55] and allow for suitable interactions with catalyst precursor species. On the flip side, these surface species cause interruptions in the graphitic structure and lead to very poor electronic conductivity.[56] Through this approach however, platinum nanoparticles and GO can be simultaneously reduced using chemical treatments (*i.e.*, with $NaBH_4$)[57–59] or solvothermal processes.[60] Interestingly, it also appears that using a thermal treatment to simultaneously exfoliate and reduce GO[61] will result in rGO with surface properties that are favourable to the deposition of well dispersed platinum nanoparticles.[19,62,63] In our previous work[19] we found that rGO prepared by this process had a surface oxygen content of 7.49 at% using X-ray photoelectron spectroscopy (XPS) that we speculated were nucleation sites for well-dispersed *ca.* 2.25 nm particles.

Using graphene-based materials that had been functionalized with carboxylic species and obtained from a commercial supplier, Tan *et al.*[21] deposited platinum and platinum nickel nanoparticles on the surface with a CO reduction process. The authors then impregnated their graphene nanosheet–platinum (GN–Pt) catalysts with an ionic liquid (IL, [MTBD][bmsi]). This IL is protic with high oxygen solubility, while being less methanol-philic than water/aqueous electrolytes. Through this approach, the prepared GN–Pt–IL demonstrated a very impressive platinum mass-based activity of 320 mA mg_{Pt}^{-1} and an even higher activity of 870 mA mg_{Pt}^{-1} for GN–Pt_3Ni–IL at 0.9 V *vs.* reversible hydrogen electrode (RHE) in 0.1 M perchloric acid ($HClO_4$). The authors believe that the graphene-based supports are able to entrap the IL due to its two dimensional structure and hydrophobic interactions between the two species. This is evidenced by significant ORR activity enhancements and mitigation of methanol poisoning effects (due to the propensity of methanol to remain in the aqueous electrolyte phase) upon addition of the IL to the catalyst. These results are likely relatable to the work of Snyder *et al.*,[64] who showed that the IL [MTBD][beti] impregnated nanoporous platinum–nickel catalysts provided ORR activity that rivalled the best single-crystal catalysts reported at the time. It is highly possible that the scaffold arrangement formed by two-dimensional platinum nanoparticle decorated graphene sheets can exhibit an IL confinement similar to these nanoporous metallic catalysts. This suggests that different combinations of IL with graphene-based materials holds promise for further performance advances, and the three-dimensional scaffold structures can likely be leveraged to induce confinement effect. Further investigations in these areas are suggested.

One difficulty in exclusively elucidating support effects in graphene-based catalysts is in that the specific synthetic techniques employed will have a large impact on the size and morphology of the nanoparticles. These parameters are well known to play a role in governing ORR activity[65,66] and serve to confound direct ORR activity comparisons between different catalyst supports. To avoid these influences, Guo *et al.*[67] separately prepared *ca.* 7 nm diameter polyhedral platinum–iron nanoparticles with controlled size and morphology. The nanoparticles were then deposited on rGO (obtained by reduction of GO by

refluxing in DMF) or carbon black by a solution phase self-assembly. In this regard, the platinum–iron particles dispersed on rGO showed an improvement in ORR activity in 0.1 M $HClO_4$ in comparison to both the carbon supported particles prepared as comparison and commercial Pt/C (from the Fuel Cell Store). In addition to excellent electrochemical stability (after 10 000 cycles from 0.4 to 0.8 V *vs.* Ag/AgCl at 100 mV s^{-1}), the rGO supported catalyst showed much higher double layer capacitance in the cyclic voltammetry (CV) profile. This is commonly reported when using graphene-based catalyst supports[19,20] and highlights the fact that graphene can provide higher electrochemically accessible surface areas than conventional supports.

A well-recognized issue with graphene materials is its propensity to "restack" through the strong pi–pi surface interactions,[68] especially during sample drying. The ultimate result is an agglomerate structure that is impenetrable to mass transport of reactive species, even when platinum nanoparticles are present on the surface.[69] Xin *et al.*[69] demonstrated that using freeze drying to collect platinum/graphene catalyst samples can allow them to be easily re-dispersed in catalyst inks. Freeze drying however may not be a feasible process for preparing fuel cell electrodes that require the deposition of a catalyst ink onto an electrolyte membrane or gas diffusion layer, followed by solvent removal. Restacking of graphene-based catalysts in this regard will result in oxygen inaccessibility through the entire catalyst layer and issues with product water removal. Li *et al.*[70] investigated this effect during ring disk electrode (RDE) preparation and devised a procedure to prevent graphene agglomeration. By mixing platinum-reduced graphene oxide (Pt/rGO) catalyst with carbon black, they showed improved ORR performance in 0.1 M $HClO_4$. Particularly, Pt/rGO did not display a well-defined mass transport limited current density at electrode potentials below *ca.* 0.8 V *vs.* RHE, which is a common feature for high surface area platinum catalysts. With the addition of carbon black into catalyst ink (and resultant electrode structure), mass transport limitations were effectively mitigated, although the catalyst did not perform as well as commercial Pt/C. An interesting feature of this work is that the authors found that ECSA losses as a result of electrochemical cycling (20 000 cycles from 0.6 to 1.1 V *vs.* RHE in air at 100 mV s^{-1}) could be dramatically hindered by the incorporation of carbon black in the electrode structure. Based on post-characterization of the catalyst, the authors claim that the carbon black can act as a trap that can anchor and nucleate any dissolved platinum species that would otherwise migrate into the bulk electrolyte solution. The common trend through investigations of this nature is that graphene-based catalysts will likely be faced with mass transport difficulties when incorporated into an electrode structure. There is therefore ample opportunity for innovative electrocatalyst and electrode engineering strategies to be designed to address these.

It would be of significance if the performance and stability improvements achieved through half-cell testing with the addition of carbon black to the catalyst ink can be translated to MEA operation. This would most certainly provide an attractive approach to exploit the unique features of graphene under practical fuel cell conditions. Jyothirmayee Aravind *et al.*[71] investigated the use of solar exfoliated graphene–CNT composites as platinum nanoparticle supports (Fig. 3a). Through half-cell experiments they found that the composite support provided higher platinum utilization (82%, based on the ratio of measured ECSA and calculated specific surface area) in comparison to using just graphene-based (49%) or CNT supports (70%). As it can be seen from transmission electron microscopy (TEM) imaging in Fig. 3b and c, despite having a slightly larger average platinum nanoparticle size (2.81 nm *versus* 2.10 nm), the Pt/G–CNT composite provides a maximum power density of 675 mW cm^{-2} in a single cell H_2/O_2 MEA, superior to 355 mW cm^{-2} for the Pt/G catalyst (Fig. 3d). This was attributed

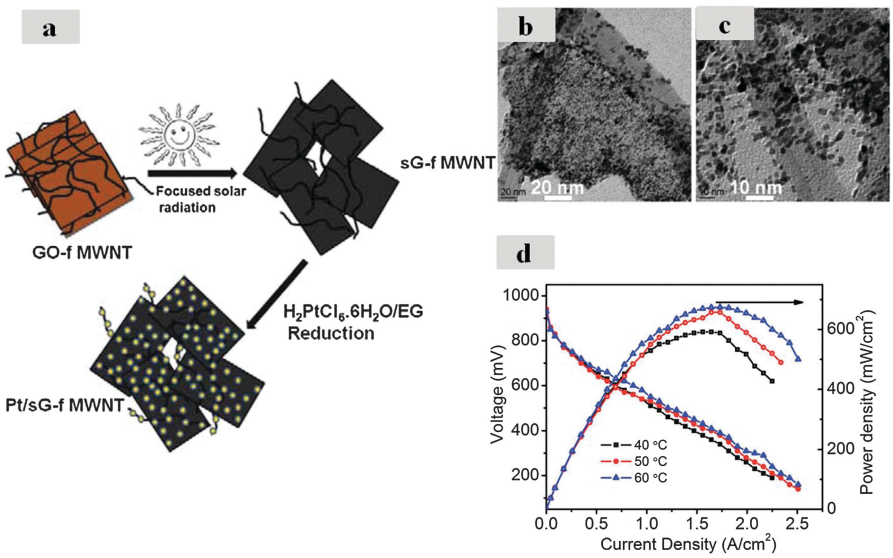

Fig. 3 (a) Illustration of Pt/sG-f MWNT preparation. (b) Low and (c) high magnification TEM images of Pt/G-CNT. (d) H_2/O_2 MEA test data for Pt/G-CNT without back pressure at different temperatures. Reproduced from ref. 71 with permission of The Royal Society of Chemistry.

to enhanced electronic and mass transport within the electrode, facilitated by the interconnected, highly conductive CNTs that act as spacers between the graphene-based materials. The maximum power density could be improved further 781 mW cm^{-2} with the application of 1 atm backpressure.

While many of the aforementioned studies have developed and characterized Pt/G catalysts, there has been little fundamental work done to understand how, and to what extent, the structure and surface properties of graphene-based materials influence Pt catalyst activity and stability. Factors such as the degree of reduction, sheet size and number of layers are unknown. It would also be worthwhile to compare graphene supported catalysts with other nanostructured, graphitized carbon supports such as CNT. These studies should be carried out in a non-adsorbing electrolyte (*i.e.*, 0.1 M $HClO_4$), to provide electrochemical activity data that is free from adsorbate effects that are encountered when using sulfuric acid (H_2SO_4). It is also worthwhile to understand the intrinsic electrochemical stability of the graphene supports themselves, in comparison to other carbon based supports (including conventional carbon black). Studies on bare graphene supports can be coupled with platinum–graphene composites, as the presence of platinum nanoparticles is known to catalyze increased rates of carbon support corrosion. If it can be exclusively demonstrated that suppressed carbon corrosion kinetics can be achieved on graphene support materials, and how the properties of the support affect these rates, engineering strategies can be employed for the design of new catalysts with unprecedented stability.

2.2. Platinum supported on heteroatom-doped graphene

Well known within the electrocatalysis community is the important effect that support materials have on the properties, activity and stability of nanoparticle catalysts. One method of tailoring the underlying catalyst–support interactions is to introduce heteroatom "dopants" (*i.e.*, nitrogen, sulfur) into the graphitic carbon support structures. If conducted appropriately, the beneficial influence of these dopant species is three-fold.[72] First, the heteroatom species serve as nucleation sites, allowing for the deposition of uniformly sized and well dispersed platinum nanoparticles *in lieu* of any surface functionalization procedure. Second, the dopant heteroatoms can favourably modify the electronic structure of the platinum nanoparticles. This modulates the surface properties of the platinum and can lead to ORR activity enhancements through weakened interactions with adsorbed surface species (*i.e.*, OH_{ads}). Finally, strengthened interactions between the doped carbon supports and the platinum nanoparticles can lead to a strong "tethering" effect that effectively stabilizes against dissolution and Ostwald ripening, two common mechanisms of ECSA loss. While the latter two phenomena (modified electronic properties and tethering effects) are difficult to measure and investigate directly, consistently observed enhancements in catalyst activity and stability in the presence of dopant species substantiate these claims.[19,22,72]

Nitrogen-doping of nanostructured carbons has been the most extensively investigated approach, with several reports on the beneficial impact of using nitrogen-doped CNTs (N-CNTs) as catalyst supports.[50,73–76] Scientists have more recently shifted these investigations to nitrogen-doped graphene-based materials (NG), demonstrating improved ORR activity and stability,[77–79] in addition to increased MEA performance[80] for NG supported catalysts in comparison to their undoped graphene-based counterparts. Vinayan *et al.*[81] obtained NG by heat treating (800 °C) a mixture of polypyrrole and hydrogen exfoliated rGO, and then deposited either Pt or Pt_3Co nanoparticles by refluxing in an ethylene glycol/water mixture. With an XPS determined nitrogen surface concentration of 5.9 at%, well dispersed and uniformly sized particles with an average size of 2.6 nm (Pt) and 2.3 nm (Pt_3Co) were obtained. Cathode structures were prepared by depositing the as prepared catalyst on a gas diffusion layer with a platinum loading of 0.4 mg cm^{-2}. Based on MEA evaluation using H_2/O_2 with no backpressure, improved performance for Pt/NG was obtained in comparison to commercial (E-TEK) Pt/C (512 *versus* 241 mW cm^{-2}), and for Pt_3Co/NG in comparison to Pt_3Co/C (805 *versus* 379 mW cm^{-2}). In their later work,[82] these authors showed that the maximum power density could be increased to 935 mW cm^{-2} when nitrogen-doped graphene/CNT composites were used as the Pt_3Co nanoparticle supports. In both reports,[81,82] preliminary stability analysis of the catalyst layers showed that using a cell voltage hold of 0.5 V at 60 °C, no loss in current density was observed for any of the NG-based supported catalyst after 100 hours. While this boasts promising stability that may be due to strengthened platinum-support binding energies (up to a factor of two) predicted by theoretical calculations for nitrogen dopant species, more rigorous stability investigations can allow further insight into practical stability capabilities and potential nature of enhancement.

Zhu *et al.*[22] aimed to couple the benefits of NG with the activity and stability benefits commonly observed on one-dimensional platinum materials (*i.e.*, nanowires or nanotubes) in comparison to conventional zero-dimensional nanoparticles.[83–85] These improvements result from the reduced surface energies and proportion of low coordination number surface platinum atoms that can mitigate dissolution/agglomeration processes and decrease the binding strength with ORR interfering adsorbates, respectively. Tellurium nanowires as templates were grown simultaneously with the reduction and nitrogen doping of GO using a hydrothermal treatment at 180 °C for 4 hours.[22] After thorough washing, platinum nanotubes (PtNTs) on the surface of NG (Fig. 4a–c) were obtained by a replacement reaction occurring between Pt^{+4} and the tellurium nanowires. Based on half-cell electrochemical testing in 0.1 M $HClO_4$ (Fig. 4d), the PtNTs/NG achieved a high platinum-based ORR mass activity of 350 mA mg_{Pt}^{-1} (Fig. 4e), representing an improvement over standalone PtNTs, PtNTs and NG that were physically mixed (PtNTs/NG-PM), and commercial Pt/C (JM). Furthermore, the PtNTs/NG showed excellent electrochemical stability through a durability testing protocol that involved 10 000 cycles between 0.6 and 1.2 V *vs.* RHE at 50 mV s^{-1} in oxygen saturated electrolyte. As a result of this procedure, PtNTs/NG showed only a 7 mV loss in half-wave potential (Fig. 4f) and retained over 90% of the initial ECSA (Fig. 4g).

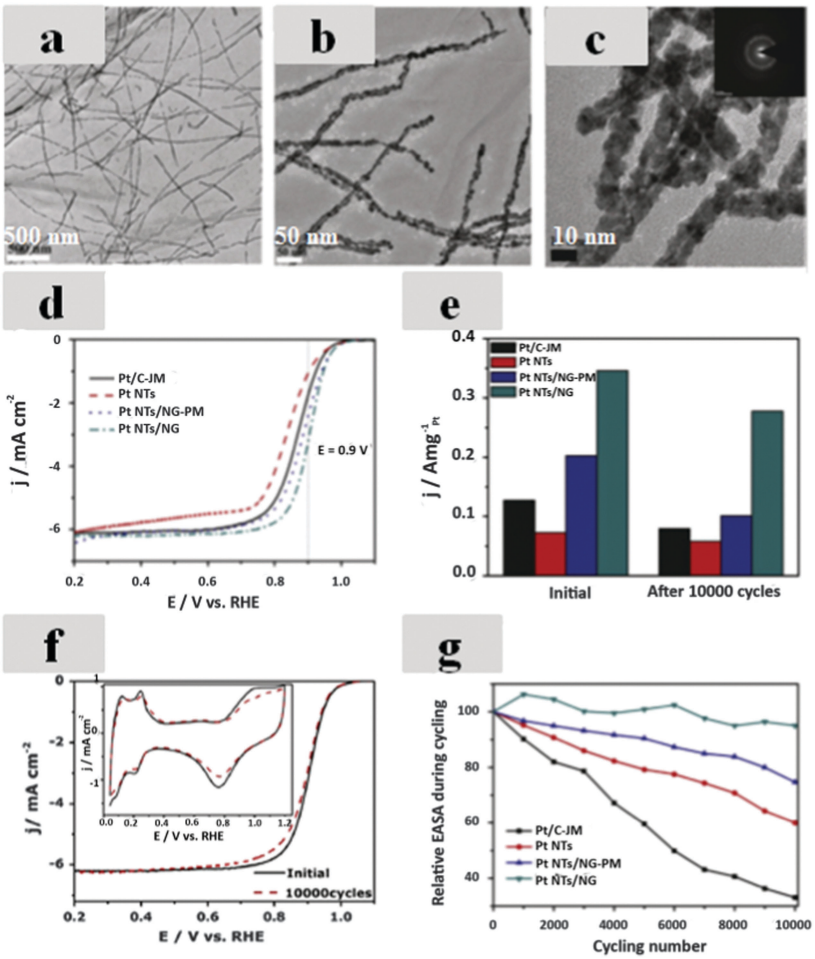

Fig. 4 (a–c) TEM images of Pt NTs/NG. (d) ORR polarization curves of the Pt NTs/NG-PM several catalysts tested as comparison in 0.1 M $HClO_4$. (e) Mass activities for the different catalysts before and after durability testing. (f) ORR polarization plots and (f, inset) CV curves before and after durability test. (g) Relative ESCA remaining for the different catalysts during durability testing. Reprinted from ref. 22, copyright (2015), with permission from Elsevier.

It is well known that sulfur and platinum can interact very strongly,[86] commonly causing issues due to surface poisoning or contamination. We speculated however that if sulfur could be immobilized within the graphitic framework of a support material, these interactions could be exploited to produce favourable catalyst–support interactions. Drawing on this, we proposed sulfur-doped graphene-based materials (SG) as a new paradigm of ORR catalyst support.[19] SG was prepared by heat treating (1000 °C) a mixture of phenyl disulfide and GO obtained by a modified Hummer's method. Undoped rGO was prepared by the same procedure, and both of these materials were decorated with platinum nanoparticles using an ethylene glycol based deposition procedure. Uniformly sized nanoparticles were successfully formed on the surface of SG (Pt/SG, Fig. 5a) and rGO (denoted as Pt/G, not shown), with average diameters based on TEM imaging of 2.10 and 2.25 nm, respectively. Sulfur was successfully doped into the structure of SG at a surface concentration of *ca.* 2.32 at%, which, based on XPS, exists primarily in the five membered ring thiophenic form (Fig. 5b). We speculate that the reduced size of the platinum nanoparticles and their excellent dispersion is facilitated by the sulfur dopant species. This is supported by our previous investigation where platinum nanowires (2–5 nm diameter) were grown on the surface of SG and rGO in an aqueous formic acid solution.[87] It was found that at low platinum loadings and using a dilute precursor solution, very uniformly sized platinum nanowires could be found on the entire SG surface, whereas growth was confined to localized islands on rGO.

The ORR activity and electrochemical stability of Pt/SG, Pt/G and commercial Pt/C (TKK) were evaluated by half-cell electrochemical testing in 0.1 M $HClO_4$. The platinum-based mass activity of the Pt/SG at 0.9 V *vs.* RHE was 139 mA mg_{Pt}^{-1}, a noticeable improvement over Pt/G (101 mA mg_{Pt}^{-1}) and commercial Pt/C (121 mA mg_{Pt}^{-1}). While this could commensurate with the differences in platinum nanoparticle size, Pt/SG displayed the highest specific activity among the catalysts investigated. This was despite the lowest average platinum nanoparticle size, which is commonly accompanied by a decrease in specific activity owing to their higher proportion of step and kink sites.[65] Most notably, Pt/SG demonstrated excellent ECSA and ORR activity retention following 1500 cycles from 0.05 to 1.3 V *vs.* RHE at 50 mV s^{-1} under nitrogen saturated conditions (Fig. 5c and d).[19] Post durability testing

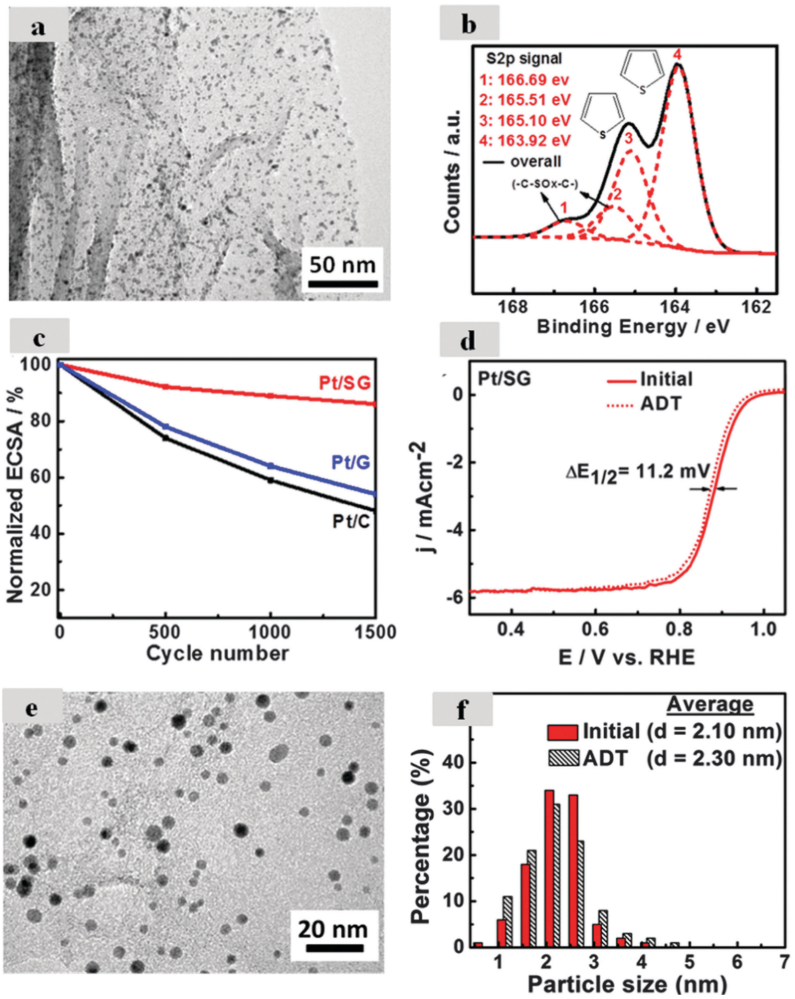

Fig. 5 (a) TEM image of Pt/SG and (b) S2p spectra of SG. (c) Normalized ECSA remaining through durability testing. (d) ORR polarization curves initially and after durability testing for Pt/SG. (e) TEM image after durability testing and (f) particle size distribution initially and after ADT for Pt/SG. Reprinted from ref. 19 with permission from John Wiley and Sons. Copyright (2014).

TEM characterization (Fig. 5e and f) revealed that the growth and agglomeration of the platinum nanoparticles on the surface of Pt was dramatically suppressed, with an increase in average size from 2.10 nm to only 2.30 nm. This was a dramatic improvement over that of both Pt/G and commercial Pt/C that demonstrated an increase in average nanoparticle size from 2.25 to 3.80 nm, and from 2.15 to 5.25 nm, respectively. To shed insight on these attractive results, we employed computational simulations to understand the interactions occurring between a model sulfur-doped graphene surface structures and both individual platinum and clusters consisting of 13 atoms. Interestingly, increased adsorptive and cohesive energies were observed between the SG and the platinum atoms and clusters, respectively, with comparison made to undoped graphene as a reference. We used this to explain the excellent platinum nanoparticle dispersion and size uniformity, in addition to the increased stability observed through half-cell investigations. The d-band centre of the platinum clusters also shifted to a more negative value when supported on SG. As a negative shift in the d-band centre with appropriate magnitude is known to result in improved ORR kinetics, we attribute this to the higher activities we observed for Pt/SG, although future investigations are needed to unequivocally validate these claims and fine-tune the support properties to achieve improved performance.

Expanding on this work, we coupled one-dimensional platinum nanowires (PtNWs) with the benefits of sulfur-doping by direct synthesis using a solvothermal procedure in the presence of SG. Micrometer length scale nanowires were successfully formed on the surface of SG, consisting of numerous single crystallites oriented in the ⟨111⟩ direction. The platinum-based mass activity of as-prepared PtNW/SG was 167 mA mg_{Pt}^{-1} at 0.9 V *vs.* RHE in 0.1 M $HClO_4$, superior to that of PtNWs grown directly on the surface of rGO (PtNW/G, 132 mA mg_{Pt}^{-1}). These catalysts were subjected to accelerated durability testing that involved 3000 cycles at 50 mV s^{-1} between 0.05 and 1.5 V *vs.* RHE, very harsh conditions that covers the potential range in which platinum catalyst degradation and support corrosion will occur in appreciable quantities.[88] Only a 22 mV loss in ORR half-wave potential was observed for PtNW/SG,[20] superior to the 86 mV loss of PtNW/G and almost complete loss of performance for commercial Pt/C. These results

once again reveal the fact that sulfur doping of graphene-based supports can play a beneficial role in catalyst activity and stability, regardless of platinum morphology (*i.e.*, nanoparticles or nanowires). For the PtNW/SG, the causation for these effects still requires further investigation, as it is unknown whether the sulfur species plays a distinct role interacting with the catalyst and/or plays a role in the platinum nucleation and growth process that provides nanowires with a morphology and surface structure that is favourable for ORR elecrocatalysis. This uncertainty is also relevant for the previously discussed PtNTs/NG catalysts,[22] whereby well-designed investigations that can prove and identify the exact effect that dopant species have on ORR performance will be crucial for uncovering knowledge that can aid in the advanced design of one-dimensional platinum/doped-graphene catalysts with unprecedented activity and stability.

Immense promise of heteroatom-doped (nitrogen and sulfur) graphene supported platinum catalysts has been reported thus far. Despite this, there are still only a limited number of research teams pursuing this approach and ample opportunity still exists to build upon the current body of work and expand scientific understanding. For example, no systematic studies exist on how different nitrogen functionalities in graphene, and their respective concentrations can impact the ORR activity and stability of deposited platinum nanoparticles. Nitrogen speciation and contents can be readily tailored by different synthetic processes and pyrolysis temperatures,[41] setting the groundwork for such studies. The same holds true for sulfur-doping, whereby the exact impact of sulfur content on the properties of graphene and resultant catalyst–support interactions remains elusive. By carefully understanding the role of these individual dopant species, it is also possible that a dual-doping approach can be used to "fine-tune" the catalyst supports to exhibit properties beneficial for ORR electrocatalysis. This notion has been demonstrated for dual-doped graphene-based materials as standalone ORR electrocatalysts in alkaline conditions (Section 4.2), providing a host of synthetic strategies to prepare these materials. Understanding how dopant species in graphene influence rates of corrosion is also an important consideration. Using nitrogen or sulfur dopants as alternatives to oxygen species for anchoring platinum nucleation and particle growth has been demonstrated. While it is known that oxygen functional groups are commonly the site for the onset of carbon corrosion, it remains to be seen if this drawback can be circumvented by the use of alternative dopants. Finally, regardless of the success in designing and developing heteroatom-doped graphene supported platinum catalysts in terms of activity and stability in half-cell electrochemical tests, fabrication into working electrode structures and their integration into MEAs for performance validation is required in order to translate any remarkable properties into practical accomplishments.

3. Graphene-based non-precious metal catalysts

To alleviate the platinum dependency of many conventional ORR catalysts, non-precious metal catalysts (NPMCs) represent an attractive class of materials that are actively under investigation. The properties of graphene can be exploited in these catalysts, including its graphitic character, high surface areas and the ability to tune its interactions with precursor species or catalytic particles. This section will discuss the role of graphene-like structures in NPMCs, including pyrolyzed transition metal–nitrogen–carbon complexes and graphene-based inorganic particle supports.

3.1. Pyrolyzed M–N–C

Presently the only ORR catalysts that are commercially available and used within acidic-based PEFCs are platinum-based. The main concern with these catalysts is their limited natural abundance and high cost that is not privy to economy of scale benefits in the same fashion other stack components are.[12–14,89] Therefore, during recent decades, numerous research teams have been focusing on the development of low cost and highly active non-precious metal catalysts (NPMCs) synthesized from readily available precursor materials as ideal platinum replacements. Successfully achieving performance and durability targets will provide enormous cost advantages to fuel cell[12,13] and metal air battery[90] commercialization efforts.

Various synthetic approaches have been applied to develop alternative catalysts,[12,13] such as the use of metal–organic framework precursors,[91] the sacrificial support method[27,92–94] and polymerization of nitrogen containing monomers (*i.e.*, aniline).[26,89,95–97] Combined with iron and/or cobalt precursors and a heat treatment at high temperature, these transition metal–nitrogen–carbon complexes (M–N–C) have been deemed the most promising class of NPMC to date. Unfortunately, these M–N–C catalysts still suffer from insufficient activity and stability during operation that pales in comparison to platinum-based materials. It is well understood that the performance of these NPMC catalysts is directly linked to the nanostructure,[89] providing opportunity for graphene and its related structures to provide advances to the current state of technology. With respect to the role of graphene in M–N–C catalysts, it is important to differentiate the two ways that graphene-based materials can be incorporated into the structure. The first is by graphene-based structures that are formed *in situ* (either deliberately or not) during catalyst preparation.[26,89,95,97–101] The second is by directly using graphene or graphene oxide as a carbon support material included in the precursor mixture that is subject to high temperature pyrolysis.[89,102–111]

Wu *et al.*[89,95,97] have shown that their developed approach to prepare M–N–C catalysts using polyaniline (PANI) as a nitrogen precursor is capable of forming a high proportion of nitrogen-doped graphene-like structures during the pyrolysis step. This can only be accomplished when a transition metal precursor is included in the reaction mixture, with a higher abundance of graphene-like sheets observed when using Co in comparison to Fe. The ability of PANI to form graphene-based structures likely arises due to the similarity between the aromatic structures of PANI and graphene.[89,95,97] Other carbon–nitrogen precursors, for example amine-based ethylenediamine (EDA)[112] or melamine[110] mostly formed carbon nanotube structures. In addition, the type

of carbon support used during PANI-based catalyst preparation influenced the formation of graphene-like structures. When using multi-walled carbon nanotubes (MWNT), a large portion of graphene "bubbles" were observed in the PANI–Fe–MWNT catalyst (indicated with green arrows in Fig. 6a).[97] When using Ketjen carbon black as a support, the formation of graphene-like structures was less prevalent as seen in Fig. 6b. Interestingly, the abundance of graphene structures was partially credited for the increased current density at a low MEA voltage (Fig. 6c) owing to the high surface areas and excellent conductivity. Improved MEA stability, investigated by holding the cell potential at 0.4 V for up to 550 hours (Fig. 6d) was also demonstrated. A relatively stable current density of *ca.* 0.3 A cm^{-2} was maintained for PANI–Fe–MWNT. This increased stability in comparison to the other carbon black supported catalysts was also attributed to the abundance of graphene sheets and bubbles. This is consistent with these authors previous report that linked increased catalyst stability with the emergence of graphene-like structures.[95]

Li *et al.*[98] developed ORR electrocatalysts based on CNT–graphene (NT–G) complexes. These were prepared through partial oxidation of CNTs, followed by high temperature heat treatment in ammonia at 900 °C for 30 minutes. The outside walls of CNTs, under certain oxidation circumstances, were moderately unzipped, forming nanosize graphene sheets (Fig. 7a and b). These graphene sheets had a small portion of iron from the CNT precursors that, in combination with nitrogen atoms, formed surface species with good activity in both alkaline and acidic conditions. The NT–G catalysts showed ORR activity close to that of state-of-the-art Pt/C in 0.1 M KOH (Fig. 7c). The onset potential was 1.05 V *vs.* RHE and half-wave potential estimated to be 0.89 V *vs.* RHE, in addition the amount of HO_2^- species formed being under 3.5% of the reduction products. In 0.1 M $HClO_4$, an onset potential of 0.89 and half-wave potential of 0.76 V *vs.* RHE were observed (Fig. 7d), very promising NPMC performance metrics at the time. This graphitized structure did not only improve the activity, but also provided enhanced corrosion resistance. After 8000 cycles between 0.6 and 1.0 V *vs.* RHE at 50 mV s^{-1} under oxygen saturated 0.1 M $HClO_4$, a small half-wave potential loss of 17 mV was detected, which was a marginal improvement over Pt/C that demonstrated a 20 mV loss.

The alternative to *in situ* formed graphene structures is using graphene or graphene oxide directly as a carbon support mixed together with nitrogen and transition metal precursors.[89,102–111] Zhang *et al.*[110] reported a facile synthesis of an Fe-doped composite of CNTs grown on and between graphene sheets. This was accomplished simply by mixing GO precursors with melamine and iron salt, followed by heat treatment in argon at temperatures between 700 and 1000 °C for 1 hour. Through this method, they found that iron could catalyze the growth of CNTs from melamine directly on the surface of the reduced GO. This method allowed for an excellent dispersion of CNTs and rGO, and also provided suitable nitrogen doping and Fe–N_x coordination that is favourable for ORR performance. In 0.1 M $HClO_4$, this hybrid structured catalyst showed good ORR activity with a well-defined

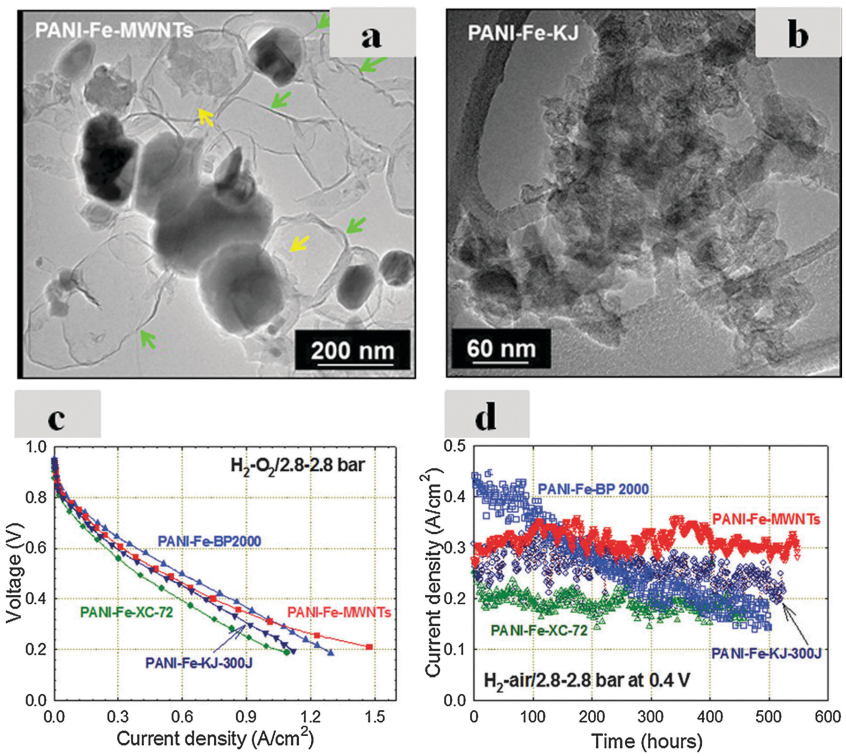

Fig. 6 TEM images of (a) PANI–Fe–MWNTs and (b) PANI–Fe–KJ. (c) Initial H_2–O_2 MEA polarization plots and (d) fuel cell durability testing. Reproduced from ref. 97 with permission of The Royal Society of Chemistry.

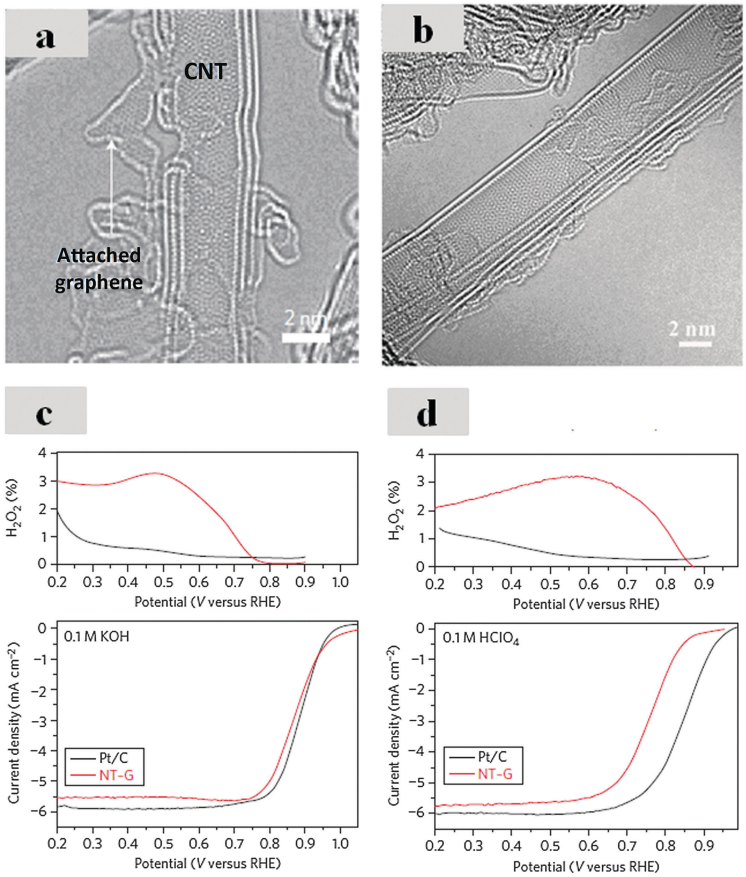

Fig. 7 (a and b) TEM images of NT–G catalysts showing the exfoliated graphene pieces attached to CNTs. Rotating ring disk electrode (RRDE) polarization curves and peroxide yield of NT–G in (c) 0.1 M KOH and (d) 0.1 M $HClO_4$. Reprinted in adapted form by permission from Macmillan Publishers Ltd[98] copyright (2012).

mass transport limited current. The half-wave potential was estimated to be 0.79 V *vs.* RHE, putting it on par with some of the best NPMCs reported to date.[27,91,95]

Despite several efforts to improve the ORR performance of M–N–C catalysts in acid, they still suffer from poor activity in comparison with Pt/C. On the other hand, activity of non-precious ORR catalysts could reach similar to or even superior over commercial Pt/C in alkaline electrolytes.[113] This is therefore an attractive research topic and is an area in which graphene-based materials can play a crucial role. Parvez *et al.*[114] used Hummers' derived GO that was modified with an anionic surfactant to enhance the interactions with the nitrogen precursor, cyanamide. These materials were all mixed in an aqueous solution, after which the water was removed leaving the dry precursor mixture. The proceeding fabrication process involved two steps, where the first step was the formation of carbon nitride by annealing in argon at 550 °C for 4 hours. Following this, the samples were then further heat treated at a temperature between 800 and 1000 °C. This allowed for the decomposition of the carbon nitride, leaving only graphene-structured materials successfully doped with nitrogen species. A pyrolysis temperature of 900 °C was deemed optimal, and in 0.1 M KOH this catalyst demonstrated an estimated half-wave potential of −0.18 V *vs.* Ag/AgCl, 3.70 electrons transferred per oxygen molecule (at −0.40 V *vs.* Ag/AgCl) and excellent methanol crossover tolerance. Furthermore, the electrochemical stability was investigated by 10 000 potential cycles between 0.2 and −1.2 V *vs.* Ag/AgCl in oxygen saturated electrolyte. The optimal catalyst showed only a 13% loss in kinetically corrected current density at −0.15 V *vs.* Ag/AgCl. This study shows the benefit of using surface functionalized GO as a carbon support structure to facilitate excellent dispersion of precursor materials and resultant active site structures. Further investigations may focus on the interactions occurring between GO, surfactant species and the associated nitrogen/iron precursors, along with the effects it has on catalyst structures and properties after high temperature heat treatments.

In spite of the valuable progress made towards pyrolyzed M–N–C non-precious catalysts, the multi-step heat treatments result in highly heterogeneous structures. This confounds investigations aimed at active site structure elucidation, and renders M–N–C catalyst development efforts as more of a trial and error approach, as opposed to rational design strategies. For this reason, it is also highly desirable to pursue the investigation of non-pyrolyzed NPMC alternatives. Transition metal N_4-macrocycle complexes supported on graphene, such as graphene-iron phthalocyanine (g-FePc)[115–117] have been prepared. For these unpyrolyzed catalysts, it is well known

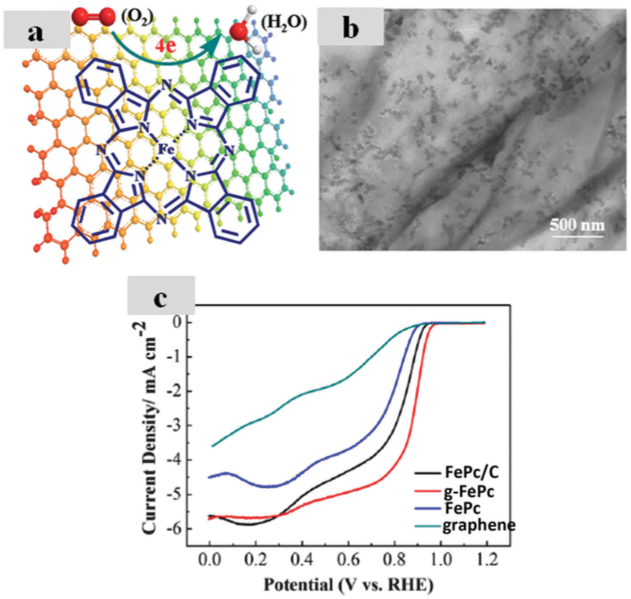

Fig. 8 (a) Schematic of the interaction between FePc and graphene (g-FePc) and the ORR happening on g-FePc (b) TEM of g-Fe-Pc and (c) comparison of FePc/C and g-FePc in 0.1 M KOH at 1600 rpm. Reprinted in adapted form with permission from ref. 115 copyright (2013) American Chemical Society.

that the activity depends mainly on the core metal type, the surrounding ligand, and the supporting material. To this end, the extended sheet structure of graphene can geometrically serve as an attractive host to these planar, two dimensional macrocycles (Fig. 8a). Furthermore, the pi–pi interactions occurring between these species can provide enhanced interaction strengths and facilitate the uniform distribution. In one example, Jiang *et al.*[115] prepared chemically reduced graphene, upon which FePc was uniformly immobilized. TEM imaging in Fig. 8b shows the homogeneous dispersion of FePc clusters decorating the surface of rGO. The use of rGO as a support improved the dispersion of non-soluble Fe-Pc, and furthermore acted as an additional electron source to compensate any issues with slow electron transfer. The resultant g-FePc displayed superior ORR activity in comparison to carbon black supported FePc (FePc/C) and unsupported FePc in 0.1 M KOH, as shown in Fig. 8c. These results corroborate the importance of carbon support structure and highlight that graphene is a highly suitable host for transition metal macrocycle complexes. While it is unlikely that even graphene supported macrocycles can provide sufficient ORR activity and stability in acidic solutions, graphene provides an ideal support structure and interactions. This can be used to overcome dispersivity issues and poor macrocycle–support interactions, enabling fundamental investigations that can provide insight into the activity of M–N–C complex NPMCs. It is clear that graphene can play a pivotal role in model electrocatalyst investigations owing to its two-dimensional and interactive nature.

3.2. Graphene-inorganic particle nanocomposites

The role of graphene in oxygen reduction catalysis can also be as a catalyst particle support. One class of NPMC that has arisen on the forefront of material science and technology is nanostructured metal chalcogenides.[118] Owing to their remarkable phase-dependant magnetic, electronic, and catalytic properties, cobalt sulfide structures has emerged as ORR electrocatalysts with the highest activity in acidic electrolyte among all other non-precious metal-based chalcogenides.[119,120] During ORR, using nanostructured support materials such as graphene is necessary in order to avoid metal oxide or sulfide nanoparticles from dissolving and agglomerating.[121] Wang *et al.*[119] obtained a new cobalt sulfide-graphene-based catalyst *via* a double-step synthesis, including a low-temperature solution-phase reaction followed by a high-temperature pyrolysis. The resulting structure

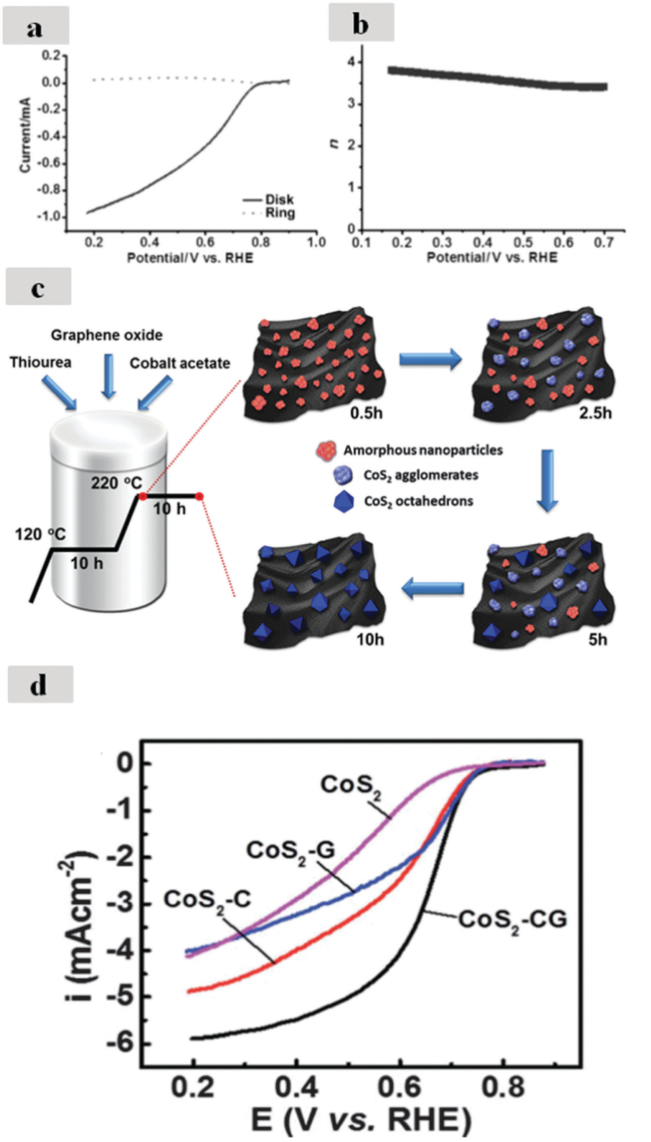

Fig. 9 (a) RRDE results and (b) electron transfer number *n* of $Co_{1-x}S$/RGO in oxygen saturated 0.5 M H_2SO_4. Reprinted from ref. 119 with permission from John Wiley and Sons. Copyright (2011). (c) Schematic of the growth of CoS_2 octahedron nanoparticles supported on N and S doped graphene. (d) ORR curves of CoS_2 catalysts supported on different nanostructured carbon supports at 1600 rpm in 0.1 M $HClO_4$. Reproduced in adapted form from ref. 120 by permission of The Royal Society of Chemistry.

consisted of mixed-phase $Co_{1-x}S$ nanocrystals supported on the surface of rGO. According to both RDE and RRDE measurements (Fig. 9a and b, respectively), a current density that steadily increased at decreasing electrode potentials was observed along with an increasing propensity for the overall four-electron ORR mechanism.

More recently, we reported a unique single step solvothermal strategy to synthesize shape controlled octahedral cobalt disulfide nanoparticles supported on nitrogen and sulfur-doped graphene/CNT composites.[120] Nanoparticle growth on individual CNTs and GO was also investigated, and a time dependent synthesis investigation revealed the growth process of CoS_2 octahedrons as depicted in Fig. 9c for the case of graphene-based supports. The presence of GO (or GO/CNTs) during the catalyst synthesis was essential, as in the absence of these nanostructure supports only large CoS_2 agglomerates were formed. Furthermore, we used GO prepared form Hummers' as a precursor, which was found to undergo reduction in addition to nitrogen and sulfur doping during the solvothermal process. The impact of support structure was readily apparent through ORR activity investigations in 0.1 M $HClO_4$ (Fig. 9d). The CNT/rGO supported CoS_2 octahedra (CoS_2-CG) outperformed all other samples, including the unsupported CoS_2 agglomerates, and rGO or carbon nanotube supported particles (CoS_2-G and CoS_2-C, respectively). Demonstrating an onset and half-wave potential of 0.78 and 0.66 V *vs.* RHE, respectively, these CoS_2-CG catalysts are the highest activity transition metal chalcogenides reported to date. The benefits of using graphene-based composite support structures were clearly revealed and future efforts should focus on understanding the nature of these enhancements to exploit them for different types of graphene supported catalysts.

Other cobalt sulfide/graphene-based catalyst investigations have also been reported. Mahmood *et al.*[122] studied the multifunctionality of a Co_3S_4/G chalcogenide composite towards both lithium-ion battery applications and ORR electrocatalysis in alkaline solutions. Liu *et al.*[123] used a solvothermal procedure to prepare a hybrid structure consisting of $NiCo_2S_4$ nanoparticles grown on graphene-based structures. These catalysts were investigated as bifunctional electrocatalysts (both the ORR and oxygen evolution reaction) in 0.1 M KOH electrolyte. This catalyst demonstrated a half-wave potential that was 47 mV lower than commercial Pt/C. The benefit of incorporating Ni into the chalcogenide structure was also evidenced by the observed increase in ORR activity upon comparison to graphene-based Co_3S_4 particle supports. While the activity and stability of all transition metal chalcogenide structures is still far below that of conventional Pt-based catalysts, doped graphene-like materials can likely provide advantageous support properties to narrow this performance gap.

There is a large body of research on graphene supported transition metal-oxides, with an entire review paper dedicated to the different types, their physical characterization and prospective for ORR catalysis.[124] Unlike acidic electrolytes, alkaline conditions are less corrosive and more favourable for the ORR in terms of electrochemical kinetics, rendering this class of catalyst more suitable. Dai's team[125,126] have conducted several studies on cobalt oxide-graphene based materials with improved ORR activity in alkaline solutions. The Co_3O_4[125] and $MnCo_2O_4$[126] particles supported on nitrogen-doped reduced graphene oxide (Co_3O_4/N-rmGO and $MnCo_2O_4$/N-rmGO, respectively) were prepared *via* a reaction mixture of GO/ethanol and NH_4OH, combined with an aqueous solution of $Co(OAC)_2$ or $Co(OAC)_2$/$Mn(OAC)_2$, respectively. Please note the convention rmGO was selected by the authors of this work because they originally prepared the GO using a lower nominal amount of $KMnO_4$, and thus considered their final product "reduced mildly oxidized graphene oxide". This entire reaction solution was mixed thoroughly at 80 °C for 20 hours, followed by a hydrothermal reaction at 150 °C for 3 hours. The $MnCo_2O_4$/N-rmGO catalyst consisted of *ca.* 5 nm nanoparticles uniformly decorating the surface of the nitrogen-doped graphene-based support (Fig. 10a and b). The ORR activity of this material in 1 M KOH was the best among the non-platinum catalysts investigated in this work (Fig. 10c), including a $MnCo_2O_4$ and N-rmGO mixture that had been physically blended together. The average number of electrons transferred was calculated by RRDE voltammetry to be 3.9 in the potential range of 0.9 to 0.5 V *vs.* RHE, indicating high selectivity towards the four electron reduction pathway. The half-wave potential was 0.87 V *vs.* RHE, among the highest reported for metal-oxide based catalysts. X-ray absorption near-edge structure (XANES) measurements revealed covalent interactions occurring between the spinel oxide particles and the underlying rmGO supports. These results show that the nature of the graphene-based supports can have a direct

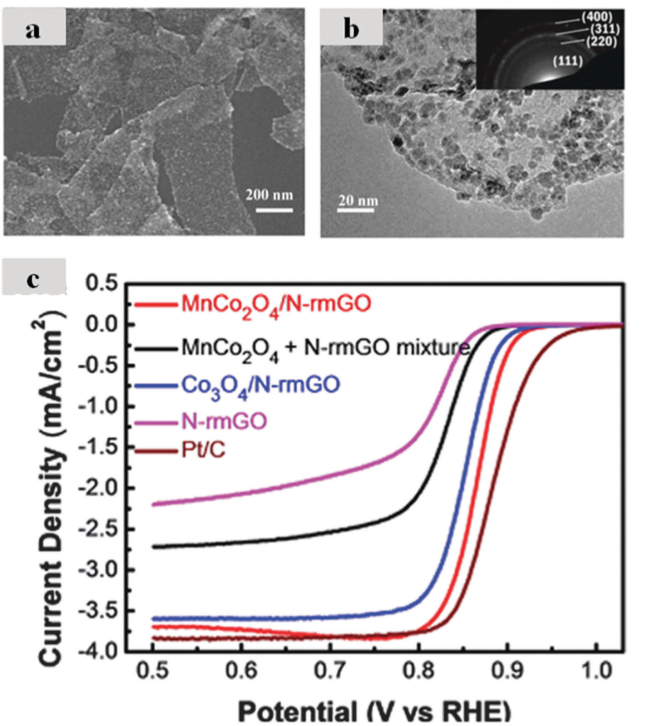

Fig. 10 Low magnification (a) scanning electron microscopy (SEM) and (b) TEM image of $MnCo_2O_4$/N-rmGO hybrid. (c) RDE results of $MnCo_2O_4$/N-rmGO hybrid, $MnCo_2O_4$ + N-rmGO mixture, Co_3O_4/N-rmGO hybrid and Pt/C in oxygen saturated 1 M KOH. Reprinted with permission from ref. 126. Copyright (2012) American Chemical Society.

influence on the electronic properties and corresponding catalytic activity of supported inorganic particles. It therefore paves the way to future design efforts aimed at tailoring the properties of graphene (through morphology control or incorporation of dopant/functionalizing species) to obtain improved ORR activities.

A wide range of other metal oxides, including Mn_xO_y,[121,127–130] Fe_xO_y,[131] and Cu_xO_y,[132] supported on graphene-based materials have also been reported to show promising ORR activity. Particularly, the unique mixed valence state of Mn_3O_4 (the simultaneous presence of Mn^{2+}, Mn^{3+}, and Mn^{4+}), which may ease the defect sites formation by introducing supplementary vacancies, holes and electrons, and would affect the electronic distribution between graphene-based structures and Mn_3O_4, making it a suitable candidate to be used as catalyst.[121] In spite of the great progresses in the synthesis of nanostructured graphene–inorganic metal oxide nanocomposites, there are still challenges to overcome. Future studies should focus on advanced synthetic strategies and not just rely on the current techniques. In the case of nanomaterials, close attention is needed to the particle size, specific surface area and phase purity. Finally, material engineering and understanding the underlying causes to the synergetic chemical coupling effects when using these nanocomposite hybrid materials can be beneficial.

4. Heteroatom doped graphene catalysts

Based on the intrinsic advantages of graphene-based materials that have been repeatedly referred to throughout this paper, there is a large body of work done on graphene-based materials and their applicability as standalone electrocatalysts towards the ORR. In particular, graphene (and numerous other high surface area carbons) has very limited activity towards the ORR, demonstrating selectivity towards the unfavourable two electron reduction mechanism. For these reasons, there is a large body of work done on graphene that has been doped with heteroatoms, with nitrogen the most commonly investigated dopant species.[41]

There exists contention within the scientific community as to what the exact active site structure are in these doped graphene catalysts. The most ubiquitous debate is whether or not metal species are an integral part of the active site structures and geometries. This issue is most critical in acidic electrolytes, where very few supposedly metal-free catalysts have been developed, and the ones that have, trail the activity of state-of-the-art materials by a significant margin. In alkaline conditions where the ORR process is more kinetically favourable, it has become broadly accepted that there are likely different or additional active site structures at play, with a large number of investigations claiming it is due to nitrogen-doped carbon structures.

This section focuses on standalone graphene-based catalysts as ORR catalysts. Put another way, this section excludes catalysts that consist of graphene-based inorganic particle supports (discussed in Section 3.2), or graphene-based catalysts that have been intentionally combined and heat treated with iron/cobalt and nitrogen precursors (*i.e.*, the M–N–C catalysts discussed in Section 3.1). Because it is becoming increasingly apparent that ORR activity in acidic conditions is very difficult to achieve without the addition of iron and/or cobalt, this section primarily pertains to alkaline conditions, such as those employed in alkaline-based fuel cells or metal–air batteries.

It is important to note that throughout the literature and in the case of some of the work reviewed within herein, many of these graphene-based catalysts are deemed "metal-free". These claims generally pertain to the fact that transition metal precursors have not been intentionally added into the precursor mixture prior to pyrolysis or alternative processing steps. Therefore, while not being intentionally misleading, the metal-free claim can often be compromised owing to trace impurities within the precursors. The most typical example is when using GO precursors that have been prepared by the Hummers' method,[44] which involves the use of transition metal containing $KMnO_4$ as a strong oxidant. While at first notion this may seem like a negligible consideration, trace metal impurities have been shown to have a beneficial impact on ORR activity[133–135] and serve to confound investigations aiming to identify active site structures in these supposes metal-free catalysts. The excellent progress made in this field of research notwithstanding, it is suggested that a degree of caution is exercised with relation to metal-free claims, unless these claims can be substantiated by inductively coupled plasma (ICP) spectroscopy or other suitable characterization.

This section will first discuss the large body of work that has been done designing, developing and implementing nitrogen-doped graphene as an ORR electrocatalyst. Expanding on this work, several research teams have highlighted the additional activity enhancements that can be gained by incorporating a second dopant element into graphene, which will be the focus of the proceeding subsection. Finally, recent efforts pertaining to the development of doped graphene/nanostructured carbon composites will be discussed in the last subsection, with prospective pathways for moving forward in this important area of research discussed. It should be mentioned that state-of-the-art non-PGM electrocatalysts for alkaline conditions still incorporate large iron contents.[136] The activity of this carbon nanotube/nanoparticle catalyst included a half-wave potential of 0.87 V *vs.* RHE at a loading of 0.2 mg cm^{-2}, and can be improved to 0.93 V *vs.* RHE with an increase in loading to 1.0 mg cm^{-2}. The objective of the work discussed in this section is to meet, or exceed the performance of these iron-based catalysts, while ideally reducing the metal dependency.

4.1. Nitrogen-doped graphene

Since Qu *et al.*[137] first reported the preparation of NG using chemical vapour deposition and its potential as an ORR electrocatalyst, many studies have followed suit in attempts to prepare highly active NG.[2,61,138–141] One intrinsic advantage of NG is that it can be produced from inexpensive, environmentally abundant precursors.[142] By eliminating the transition metal dependency of several ORR catalysts, catalyst production can

become more favourable from a sustainability perspective.[143] A good example is the work of Pan *et al.*,[144] whereby these authors prepared NG catalysts by pyrolysing (between 800 and 1000 °C) a mixture of crystal sugar and urea. After heat treatment, a crumpled, multilayered graphene structure was observed (Fig. 11a–c). The authors claim that this structure arises due to the propensity of urea to form graphitic carbon nitride in the 350 to 550 °C range. At temperatures in excess of 800 °C, this graphitic carbon nitride decomposes, serving as a sort of template that is both formed and decomposed during a single heat treatment process. The catalyst prepared at 1000 °C with a surface area of 565.1 $m^2 g^{-1}$ displayed the highest ORR activity among the other preparation temperatures (Fig. 11d). A half-wave potential of *ca.* −0.14 V *vs.* Ag/AgCl was achieved in 0.1 M KOH, along with a well-defined mass transport limited current density and electron transfer number of 3.8 determined by Koutecky–Levich analysis at an electrode potential of −0.25 V *vs.* Ag/AgCl.

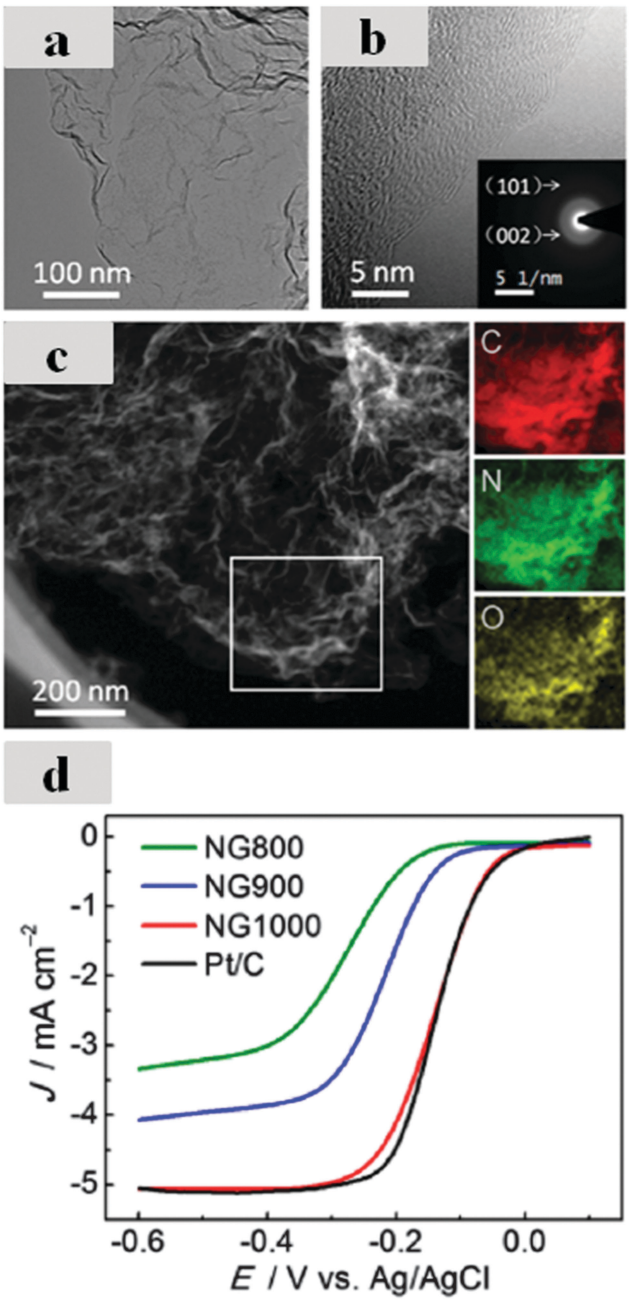

Fig. 11 (a) TEM, (b) HRTEM and (c) STEM images of NG1000. (d) ORR polarization curves of different samples and Pt/C at 1600 rpm in 0.1 M KOH. Reprinted with permission from ref. 144. Copyright (2013) American Chemical Society.

In another report, Geng *et al.*[138] prepared NG materials by heat treating GO in an ammonia/argon environment. This method is attractive because ammonia treatment had previously been shown capable of simultaneously reducing and nitrogen doping GO,[145] with the extent of each controlled by the temperature utilized. The GO used in this work was prepared by the Staudemaier method that involves oxidizing natural flake graphite with strong acids (avoiding the use of $KMnO_4$).[138] Using an ammonia treatment temperature of 900 °C, optimal ORR activity was obtained for the NG with a nitrogen surface concentration of 2.8 at%. Notably, an onset potential *ca.* 0.26 V higher than that of undoped graphene was achieved in 0.1 M KOH, in addition to a relatively high number of electrons transferred (3.8) at −0.5 V *vs.* SHE, determined by RRDE testing.

To increase the intrinsic activity of NG catalysts, it is very worthwhile to gain a structural and mechanistic understanding of the ORR process. Several authors have drawn relationships between ORR activity and the pyridinic nitrogen content,[45,137,146,147] while others claim graphitic nitrogen is at the source of ORR activity.[148–151] Even further complicating matters, additional studies have claimed that both of these species contribute to ORR activity, with some sort of complex interplay occurring between them.[139,152] Xing *et al.*[153] recognized the uncertainty in this area that arose from the indirect experimental determinations of active site structures. To address this, the authors conducted synchrotron based XPS investigations of NG catalysts both before and after the ORR. They synthesized a series of NG catalysts from GO (prepared by the Hummers' method) using different nitrogen precursors and processing regimes. By comparing results from the high resolution N1s, O1s and C1s, it was found that the NG catalysts underwent distinct changes after the ORR, induced by cycling the electrode from 0.2 to −1.0 V *vs.* Ag/AgCl at 100 mV s^{-1} in oxygen saturated 0.1 M KOH. Particularly, a correlation could be established between the activity of the different NG and the amount of –OH groups that were chemisorbed on carbon atoms adjacent to pyridinic nitrogen. They propose that this $OH_{(ads)}$ is an adsorbed intermediate species of the ORR, signifying this carbon site serves as the active site. This is in agreement with the experimental and computation work of Gong *et al.*[32] that predicted nitrogen atoms caused a charge shift on neighbouring carbon atoms, inducing adsorptive behaviour for oxygen molecules. It was also shown that the absolute content of pyridinic nitrogen does not necessarily govern ORR activity and that there is another factor at play, which the authors speculate is the microstructure of the pyridinic sites,[153] a feature that is very difficult to determine experimentally. This study also highlights the uncertainty that can arise from XPS results; especially those

conducted using lab scale X-ray sources that can provide only a fraction of the brightness of synchrotron facilities to obtain high resolution measurements in a suitable time period. Slight changes in the surrounding environment of nitrogen atoms can change the electron binding energy and corresponding signals. The fitting techniques and parameters used to differentiate species are thereby somewhat arbitrary, and can have a big effect on the relative contents of each species.

In an attempt to maximize the formation of pyridinic (and pyrrolic) nitrogen species, Ding *et al.*[151] developed a flat, layered montmorillonite (MMT) nanoreactor with an interlayer spacing of 0.46 nm. This MMT reactor was intercalated with aniline monomer that was oxidized to polyaniline with the addition ammonium persulfate. The mixture with a lamellar structure consisting of alternating layers of MMT/polyaniline was then heat treated at 900 °C in argon for 3 hours, followed by MMT removal using hydrofluoric acid. With the fabrication depicted schematically in Fig. 12a, the authors show that the spatial confinement of the reactor design allowed for more favourable formation of pyrollic and pyridinic nitrogen with a planar structure, in favour of graphitic nitrogen with a three-dimensional tetragonal configuration. In fact, when polyaniline was heat treated in the absence of MMT, 70.2% of the overall nitrogen atoms were either graphitic or oxidized nitrogen species, and this value was decreased to 9.73% when the MMT was employed. Additionally, this method allowed for higher overall nitrogen contents than those obtained in the absence of MMT. Most notably, the authors investigated the ORR activity performance of their prepared catalyst in acidic conditions. Fig. 12b shows linear sweep voltammetry results in oxygen saturated 0.1 M $HClO_4$, whereby the best performing materials (NG@H-MMT) achieved a half-wave potential of

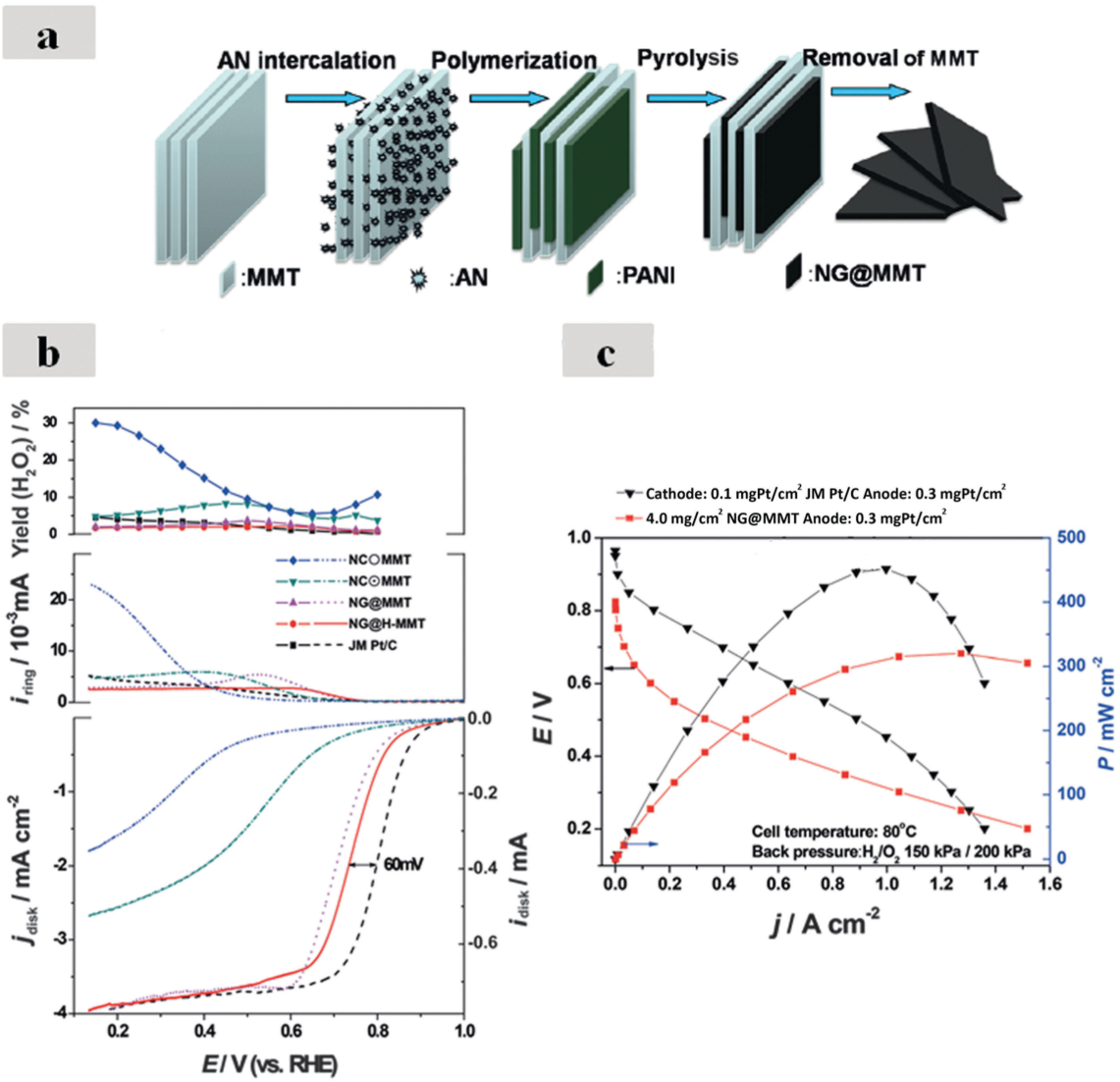

Fig. 12 (a) Schematic of the synthesis of NG@MMT. (b) ORR polarization, ring current, and peroxide yield in 0.1 M $HClO_4$. (c) Power densities and corresponding polarization curves of MEA prepared from NG@MMT. Reprinted from ref. 154 with permission from John Wiley and Sons. Copyright (2013).

ca. 0.74 V *vs.* RHE. A maximum power density of 320 mW cm^{-2} was also obtained in an H_2/O_2 cell employing a NG@H-MMT/carbon black based cathode (Fig. 12c). While the presence of trace metal impurities was not exclusively ruled out, if truly metal free this activity represents a notable accomplishment that is worthy of further fundamental investigations. It would additionally be of interest to apply a similar design approach to tune ORR activity in alkaline conditions, in addition to investigate the potential influence of sulfur-dopant species that potentially result from the use of ammonium persulfate and could provide ORR enhancement in a manner akin to the dual-doped graphene catalysts discussed in the proceeding Section 4.2.

While many studies actively probe the catalytic centres for ORR activity and develop synthetic strategies can be adopted to maximize their formation (microscopic approach),[139,152,153,155] at the other end of the catalyst design spectrum is the macroscopic approach that involves the generation of structural features and porosity that can improve active site accessibility and facilitate oxygen transport.[147,156–159] Wei *et al.*[160] prepared graphene silica templates by hydrolysis of tetraethylorthosilicate on the surface of GO prepared by the Hummers' method. This drew on the work this group did previously employing this approach in preparing high surface area nitrogen- or sulfur-doped graphene-based materials,[161] yet expanded upon it by assembling colloidal silica nanoparticles with average diameters of either 22 or 7 nm on the surface of the graphene–silica composites.[160] This entire mixture was then coated with polydopamine and subjected to a heat treatment at 800 °C in nitrogen for two hours, after which the silica templates were etched away with 2 M NaOH solution. This entire process is depicted in Fig. 13a, and found to result in nitrogen-doped carbon nanosheets (NDCN) with controlled, uniform pores (Fig. 13b) that have size control reflective of the silica template nanoparticle diameters used. Using 22 nm colloidal silica particles (NDCN-22) resulted in the highest ORR activity that is likely reflective of a BET surface area of 589 m^2 g^{-1} and pore volume of 1.52 m^3 g^{-1}. In 0.1 M KOH, NDCN-22 demonstrated a half-wave potential of −0.13 V *vs.* Ag/AgCl (data not shown), with the number of electrons transferred determined by RRDE evaluation ranging from 3.67 to 3.94 in the ORR relevant potential range. Their activity was also investigated in acidic (0.5 M H_2SO_4) electrolyte (Fig. 13c), whereby the heat treatment temperature effect was investigated and an onset and half-wave potential of 0.72 and 0.56 V *vs.* RHE, respectively was demonstrated for NDCN-22 prepared at 900 °C. This study is reflective of the large body of work done by Serov *et al.*[27,92,93] for the development of heat treated M–N–C catalysts by the sacrificial support method. Drawing on this work, it is possible that further improvement gains can be achieved by combining sacrificial particles of different sizes and shapes to achieve a mixture of meso- and macropores in the resultant electrode structures.

A significant amount of success has been realized on the use of metal organic framework (MOF) derived M–N–C catalysts for ORR electrocatalysis in acidic conditions, and most particularly

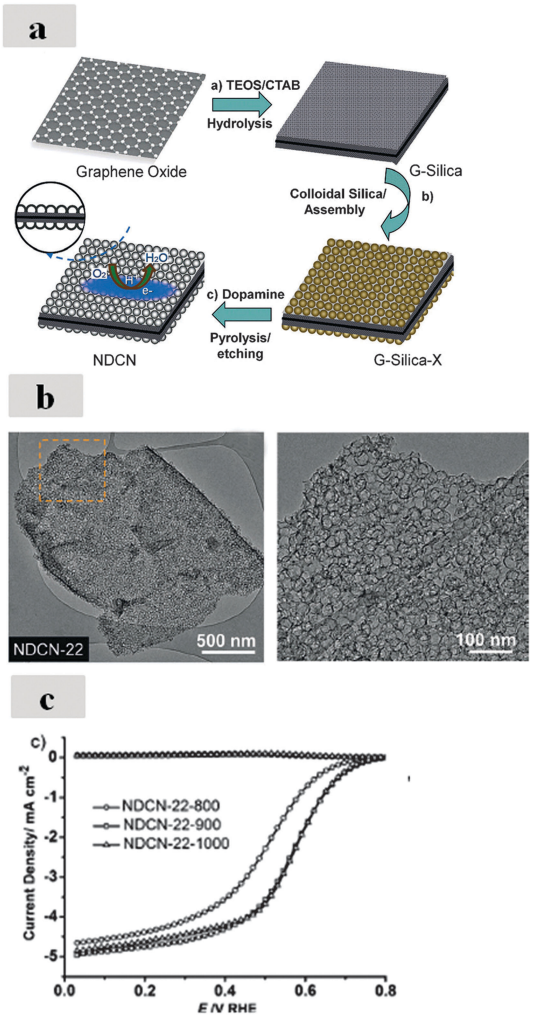

Fig. 13 (a) Schematic of NDCN synthesis. (b) TEM images of NDCN-22. (c) RRDE results in O_2-saturated 0.5 M sulfuric acid of NDCN-22 synthesized at different pyrolysis temperatures. Reprinted from ref. 160 with permission from John Wiley and Sons. Copyright (2013).

with the use of zinc centred zeolitic imidazolate frameworks (ZIF).[162,163] The benefit in using ZIFs is that they are generally very porous, have ligand structures that can serve as nitrogen and carbon sources, and during the heat treatments required for catalyst synthesis produce volatile species that can generate highly porous structures. To make a homogeneous graphene-based catalyst, Zhong *et al.*[111] employed a method to homogeneously disperse ZIF particles on the surface of GO that was prepared by the Hummers' method. They used PVP to functionalize the GO, as it provided surface species that could coordinate with the ZIF precursors and ensure uniform nucleation. This composite was lyophilized to retain its morphological features, heat treated at 800 °C in argon for 5 hours and then treated with 2 M HCl to remove any remaining metallic impurities. It is worthy to mention that while using zinc during fabrication very likely results in a residual metal content within the catalyst, zinc-species are considered inactive for the ORR and are generally reduced to minimal quantities after heat treatment and/or acid leaching processes. A very high surface

area of 911 m^2 g^{-1} was found for the graphene-based nitrogen-doped porous carbon sheets (GNPCSs). Significantly increased onset potentials were also found for the GNPCS in comparison to catalysts prepared from a physical mixture of GO and ZIF, or from the ZIF structure in the absence of GO. This successfully validated the importance of well-dispersed ZIF particles anchored on the surface of GO, although any additional roles of PVP acting as a supplementary nitrogen source or pore forming agent remains unclear. A well-defined mass transport limited current density was achieved for GNPCS, and HO_2^- production yield of less than 10% at all potentials investigated was determined both by Koutecky–Levich analysis and RRDE evaluation. The authors integrated the prepared catalyst into electrode structures with a loading of 4 mg cm^{-2} and used them as the cathode in a direct methanol alkaline exchange membrane fuel cell. The open circuit voltage (OCV) for the GNPCS cathode was 0.71 V, and it reached a maximum power density of 33.8 mW cm^{-2}. These performance metrics were superior to commercial Pt/C (Johnson Matthey) cathode (0.65 V and 22.5 mW cm^{-2}, respectively), and was attributed to the intrinsic ORR activity and excellent methanol tolerance of the GNPCS catalyst.

It is clear that excellent progress has been made in the field of NG-based catalyst development for ORR electrocatalysis, and some promising approaches for advancing this field of research will be discussed in proceeding sections. It is also becoming increasingly apparent that electrochemical evaluation of these catalysts should be standardized so that appropriate comparison can be drawn between results of different investigations. As of now, the ORR activity of numerous graphene-based materials is reported with reference made to underperforming Pt/C catalysts, thereby providing an overestimation of intrinsic performance. Additionally, different types of reference electrodes are reported throughout the literature. Ag/AgCl electrodes are a common choice, but when using alkaline electrolytes one must to consider the potential formation of silver oxide/hydroxide species within the reference electrode or glass frit that can impact measured potential values. Any drift in the potential values can confound performance results within an individual set of experiments, and make it very difficult to conduct a cross-study evaluation of catalyst performance and interpret results in the context of the current literature. It is recommended that when conducting ORR experiments, potentials are reported *versus* the RHE with the reference electrode of choice calibrated to the hydrogen equilibrium potential both before and after all measurements. The use of graphite counter electrodes should also be used in favour of platinum so that any possibility for precious metal contamination of the working electrode can be avoided. Finally, it is strongly recommended that all claims of "metal-free" catalysts be substantiated by inductively coupled plasma spectroscopy or other suitable techniques to ensure that the ORR activity is not arising due to trace metal contents introduced during catalyst preparation or through precursor impurities.

4.2. Dual-doped graphene

There are numerous investigations reported throughout the scientific literature to prepare graphene-based materials doped with alternative heteroatoms, including sulfur,[161,164–170] phosphorus,[171] boron[172,173] and iodine.[174] The unique synthetic procedures are most certainly of interest to the electrocatalysis community; however the ORR activity of these heteroatom doped graphenes still trails the best performing NG discussed in the previous section. The majority of alternative dopant catalysts display changing ORR selectivity from the non-preferred two electron reduction mechanism at low overpotentials (forming hydrogen peroxide species) towards the overall four electron reduction mechanism at high overpotentials. Such behaviour results in a pseudo current density plateau at intermediate potentials, followed by a continuous increase as the potential is lowered. This behaviour is typically observed for non-doped nanostructured carbons regularly included in activity investigations for comparative purposes and is reflective of relatively poor activity (see activity of CNT in Fig. 1 of ref. 175 or of graphene in Fig. 1 in ref. 138 for typical examples).

While possessing relatively poor activity on their own, it has been found that the incorporation of additional dopant species into nitrogen-doped carbon structures can tailor the surface properties in a fashion that is favourable for ORR kinetics.[176–180] Boron doped carbon nanostructures had previously been prepared,[103,181,182] and several authors have more recently pursued the doping of graphene-based materials with boron in combination with nitrogen (B,N-G). Wang *et al.*[183] thermally annealed GO in the presence of boric acid and ammonia, while Xue *et al.*[184] prepared three-dimensional nitrogen- and boron-doped graphene-based foams by chemical vapour deposition of melamine diborate decomposition products on the surface of a sacrificial nickel foam template. Both studies showed successful incorporation of nitrogen and boron into the graphene structures, albeit a significant portion of hexagonal boron nitride (h-BN) was observed. This is understandable as the commercial production of h-BN is conducted by high temperature combination of small boron and nitrogen containing organic molecules,[185] but the notable properties that include chemical inertness and electronic resistivity render it undesirable for electrocatalysis applications.

To avoid the formation of inactive, insulating h-BN, Zheng *et al.*[186] developed a unique two-step procedure to synthesize B,N-G. In the first step, GO prepared by the Hummers' method was thermally treated in ammonia at 500 °C for 5 hours, resulting in partial reduction and introduction of nitrogen dopant species. This material was then heat treated with boric acid at 900 °C for 5 hours. By separating the doping steps, B,N-G was prepared in which nitrogen and boron replaced carbon atoms within the graphene-based structure based on XPS (Fig. 14a). Furthermore, the formation of h-BN was completely avoided through this technique and a well-defined graphene-like structure resulted (Fig. 14b). The ORR activity in 0.1 M KOH of B,N-G (Fig. 14c) in terms of onset potential, current density and four electron selectivity was substantially improved *versus* a wide array of materials prepared for comparative purposes (including individually doped graphene- and h-BN-graphene-based materials produced with simultaneous dual doping). A near four electron reduction mechanism was determined by Koutecky–Levich analysis and RRDE measurements, and the onset and half-wave potentials

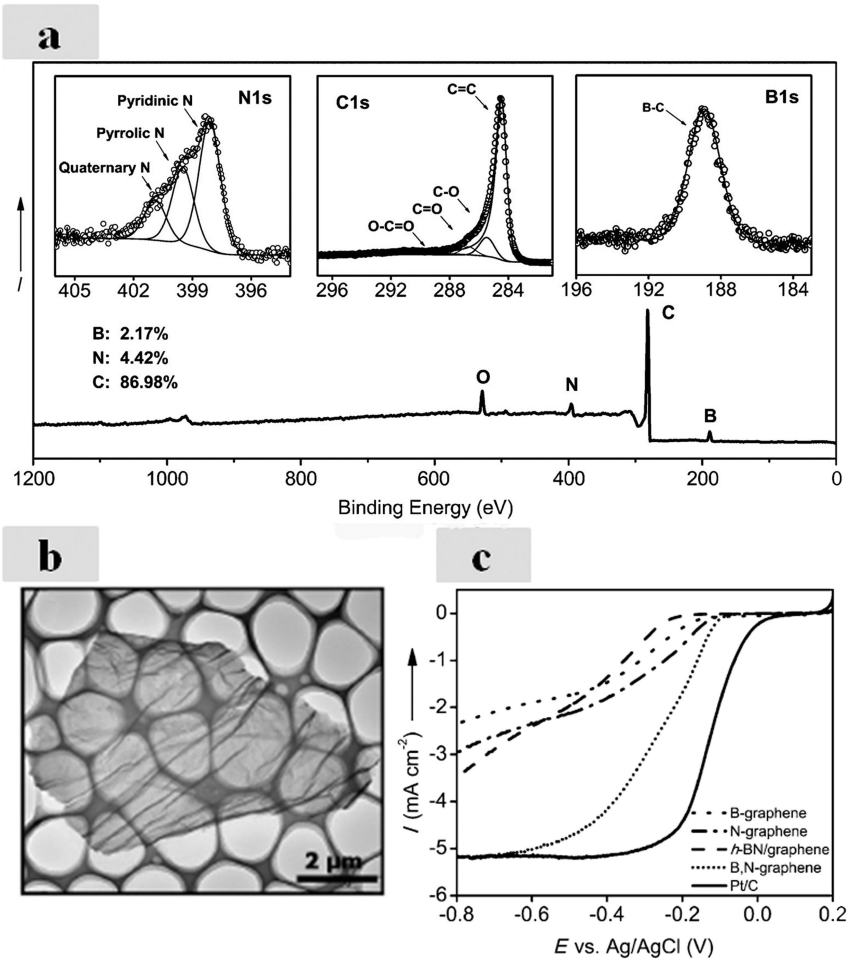

Fig. 14 (a) XPS spectra of nitrogen, carbon and boron (B1s) core levels in B,N-graphene. (b) TEM image of B,N-graphene and (c) linear sweep voltammetry (LSV) of different catalysts in oxygen saturated 0.1 M KOH. Reprinted from ref. 187 with permission from John Wiley and Sons. Copyright (2013).

for the ORR were −0.06 and *ca.* −0.25 V *vs.* Ag/AgCl, respectively. The authors also employed density functional theory (DFT) calculations to further understand the interactions between nitrogen and boron dopant species. They found a beneficial synergistic effect towards the ORR that could be tuned by changing the identity of the dopant species and microstructure of the active sites that if implemented successfully, could likely lead to improved activity.

Dual-doping of graphene with both sulfur and nitrogen (S,N-G) has also been investigated, where seemingly less potential exists to form inactive phases during preparation. The activity of S,N-G has consistently been demonstrated higher than N-G or S-G prepared by similar procedures,[176,188] highlighting the beneficial impact of this dual-doped configuration. An additional benefit of this atomic combination is that dopants can be provided from a single source precursor (*i.e.*, thiourea),[189,190] simplifying the fabrication process. Using separate nitrogen and sulfur precursors, Liang *et al.*[191] prepared mesoporous S,N-G by mixing GO prepared from Hummers' method, melamine and benzyl disulfide. Colloidal silica particles (12 nm) were also added to the mixture that was heat treated at 900 °C in argon for 1 hour, followed by hydrofluoric acid removal of the silica particles. The resulting S,N-G had a high content of mesopores ranging in size from 10 to 40 nm, and XPS determined nitrogen and sulfur surface contents of 4.5 and 2.0 at%, respectively. An onset potential of −0.06 V *vs.* Ag/AgCl was achieved for the S,N-G and the number of electrons transferred determined by Koutecky–Levich analysis ranged from 3.3 to 3.6 over the potential range investigated. The authors exclusively showed activity enhancements that arose due to dual-doping by providing comparison with N-G and S-G prepared by similar processes, albeit in the absence of benzyl disulfide or melamine, respectively. To understand this observation, DFT calculations were employed to probe the interactions occurring between dopant species. For nitrogen, the neighbouring carbon atoms with a high charge density were deemed the ORR active sites. In sulfur, with electronegativity similar to carbon, minimal charge transfer occurs and activity is thereby induced by an orbital mismatch that results in a positively charged sulfur atom proposed as the active site. When nitrogen and sulfur are simultaneously present, two things occur. First, a larger number of carbon atoms have activity due to the electronic modifications provided by the dopant species (increased number of active sites). Second, the charge and spin

densities of the atoms in S,N-G are increased, providing higher intrinsic ORR activity, with these conclusions used to explain the experimental results of this investigations. It could also be conjectured that the incorporation of sulfur-dopants in the five-fold coordinated thiophenic arrangement disrupts the lattice of graphene, providing an increased degree of edge plane exposure that has been linked to catalytic activity.[192,193]

The combination of phosphorus and nitrogen as dual dopants into carbon nanostructures has also been reported,[194] with activity enhancements observed with the inclusion of phosphorus into nitrogen-doped carbons, or into nitrogen and boron-doped carbons (note: iron and cobalt species added during synthesis). This was attributed to modified charge distributions in the carbon, in addition to the morphological effects that result in higher edge site exposure. In terms of graphene-based materials, Razmjooei *et al.*[190] investigated ternary doping with phosphorus, sulfur and nitrogen (P,S,N-G). They accomplished this by thoroughly mixing GO from the Hummers' method with thiourea and triphenylphosphine in ethanol solvent. The mixture was then dried, ground and pyrolyzed at 800 °C in nitrogen for 2 hours. The authors investigated the impact of the nominal amount of thiourea in the precursor mixture, in addition to developing undoped graphene, phosphorus-doped graphene (P-G) and S,N-G. Interestingly, the incorporation of phosphorus into the structure of P,S,N-G resulted in decreased total Brunauer–Emmett–Teller (BET) surface area, although a higher mesoporous surface area and higher capacitance from cyclic voltammetry was observed. The addition of phosphorus into graphene-based materials resulted in a 30 mV onset potential increase from −0.18 to −0.15 V *vs.* Ag/AgCl in 0.1 M KOH. Upon doping phosphorus into S,N-G, a 70 mV increase in onset potential occurred with the P,S,N-G catalyst providing the highest activity among all samples investigated, including an onset potential of −0.03 V *vs.* Ag/AgCl and an estimated half-wave potential of −0.17 V *vs.* Ag/AgCl. The HO_2^- production was also less than 10% over the entire electrode potential range investigated.

In the majority of investigations, the incorporation of heteroatom dopant species into graphene-like structures is deliberate. In other cases activity improvements can potentially be achieved by additional dopant species introduced serendipitously as a result of the chemical processes used. In one example, Li *et al.*[195] prepared nitrogen and phosphorus dual-doped graphene/carbon nanosheets (N,P-GCNS). These materials were prepared using Hummers' derived GO solution in which aniline and phytic acids were added. The aniline was then polymerized with the addition of ammonium persulfate as an oxidant, and this entire solution was mixed for 24 hours until a gel was obtained. It was then dried and heat treated at 850 °C for 2 hours in nitrogen. The derived materials had a very large surface area of 900.2 $m^2 g^{-1}$, with a large content of pores in the 0.8 to 1.2 nm and the 10 to 40 nm range. It is important to note is that sulfur is included in the reaction mixture from the ammonium persulfate added as the oxidant. It is interesting to note that no distinct sulfur signal was observed in the low resolution XPS spectra; however it is possible that sulfur species are present in amounts below the detection limit and still have an effect on the activity of the developed catalysts. In fact, previous work on cyanamide[196] or polyaniline-derived (polymerized using ammonium persulfate)[95,197] M–N–C catalysts have shown that sulfur plays a role in enhancing ORR activity. The exact role of sulfur is unknown, but the activity improvements realized for S,N-G *versus* N-G materials discussed previously shows that it is somewhat universal. Regardless, the onset potential of the N,P-GCNS was 1.01 V *vs.* RHE in 0.1 M KOH, and the importance of including both phosphorus and GO (for uniformly hosting precursor polymers) in the reaction mixture was exemplified. A half-wave potential of *ca.* 0.87 V *vs.* RHE with an almost complete selectivity towards the four electron reduction of oxygen determined by Koutecky–Levich analysis and corroborated by RRDE testing. The performance of this catalyst can thereby be considered among the best in alkaline conditions. Based on extensive characterization of the materials, the authors suggest that both the microstructure and heteroatom dopant species play an important role in the performance improvements, although the exact mechanisms are still speculative at this point in time.

A similar occurrence might be at play for the work of Lin *et al.*[150] and Mo *et al.*[198] The latter prepared thermally expanded rGO by heat treating GO prepared by the Hummers' method at 850 °C in argon. In parallel, the authors prepared polyaniline by the polymerization of aniline monomer with ammonium persulfate. The thermally expanded rGO and polyaniline were then placed in separate quartz boats inside a tube furnace that was heated up to 850 °C for 1 hour under argon flow. This process allowed for a very high BET surface area of 1119 $m^2 g^{-1}$ and significant nitrogen content of 6.27 at%. Using elemental analysis, 1.89 at% sulfur was present in the catalyst, although no sulfur peak was detected by XPS. This indicates that either sulfur is entrapped within the bulk of the catalyst, or is below the sensitivity threshold of the XPS measurements. With ORR polarization curves shown in Fig. 15, it is clear this NG (the presence of sulfur is omitted) catalyst outperforms GO, and the

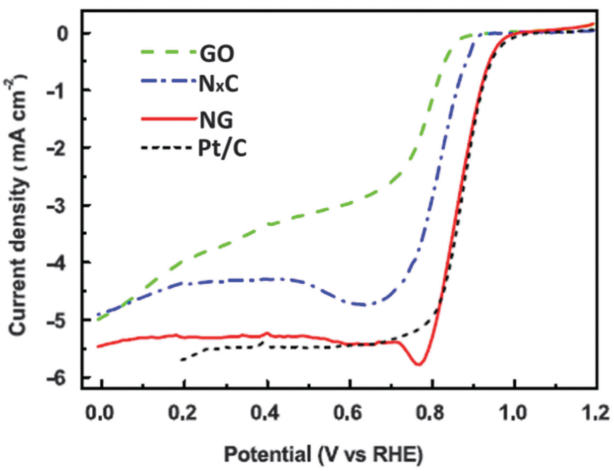

Fig. 15 ORR polarization plot for of GO, N_xC, NG and Pt/C catalysts in 0.1 M KOH at 1600 rpm. Reprinted in adapted form from ref. 198, Copyright (2015), with permission from Elsevier.

N_xC catalyst prepared simply by the pyrolysis of polyaniline. The latter sample had a surface area of only 238 m^2 g^{-1}, attesting to the importance of using graphene and the "transfer doping" approach during catalyst preparation. The onset potential for ORR was 0.98 V *vs.* RHE and the half-wave potential was estimated to be *ca.* 0.88 V *vs.* RHE, placing it as one of the best performing graphene-based catalysts amongst the materials discussed in the previous paragraph.

The studies discussed in this section have successfully showed enhancements in oxygen reduction electrocatalysis that can be achieved by dual (or ternary) doping of graphene-based structures with nitrogen seemingly the most crucial species for generating high activity. Even with several reports linking experimental and computational simulations, there is still a large degree of uncertainty surrounding the individual and synergistic roles of each dopant species within the graphene lattice. Various factors may affect the activity when incorporating dopant species, including the formation of new active sites, modulatted electronic and adsorptive properties, morphology or chemical composition changes induced by the presence of dopant species during synthesis, or changes to the microstructure of the catalyst surface. It is likely a combination of each of these factors that govern the properties and activity of resulting graphene-based catalysts, but the extent of each and mechanistic pathways remains unknown. It is prudent to conduct detailed computational simulations that are linked to surface sensitive probing techniques (both *in situ* and *ex situ*) to truly understand the roles and behaviour of the various dopant species present in graphene. If this information can be elucidated, rational design strategies can be employed to further improve performance.

There is clearly room for improvement in this class of dual-doped graphene-based catalysts. This can be evidenced by the fact that many of the nitrogen-doped graphene catalysts prepared and used for comparative purposes with dual-doped catalysts have much lower performance than the best in class nitrogen-doped graphene catalysts discussed in Section 4.1. Therefore, if the most effective synthetic strategies to prepare highly active nitrogen-doped graphene are conducive to the incorporation of a second or third type of adatom, unprecedented performance capabilities are likely. Finally, tailoring the overall structure of the dual-doped graphene-based materials to allow efficient oxygen access and product removal from the active sites could facilitate further performance gains. One strategy to accomplish this includes the development of graphene/nanostructured carbon composite catalysts that are the topic of the following section. Another strategy discussed briefly in this section is the use of sacrificial templates to generate mesoporosity. It is known that the size, shape and content of pores can govern activity, yet is readily tunable by careful template selection. Systematic investigations can be conducted to understand the exact effects and achieve optimized pore sizes and distributions for efficient electrocatalysis.

4.3. Graphene/nanostructured carbon composites

Drawing on the progress made in graphene-based catalyst research and development, it is likely that even further advancement and activity enhancements can be achieved by compositing graphene with other nanostructured carbons. Such composite arrangements can effectively couple the attractive properties of each individual constituent while simultaneously producing synergistic benefits. At the same time this approach allows one to compensate or even overcome some of the shortcomings of the individual materials. Take one-dimensional CNTs for example. They are highly conductive and have the benefit of forming interconnected, highly porous architectures that are attractive from an electrode design standpoint. On the flip side, their tubular morphology with an inaccessible core leads to reduced surface areas capable of hosting active site species. Graphene on the other hand has increased surface areas owing to its two-dimensional morphology, and highly tunable surface chemistries, especially when using GO as the starting material.[56] On its own however, graphene has the propensity to restack due to van der Waal's forces, and because of its sheet like structure causes difficulties in generating electrode architectures that are highly conducive to reactant mass transport. When composited, all of the intrinsic advantages of each CNTs and graphene still exist, in addition to the fact that the high surface area of graphene can be capitalized on because the CNTs act as electronically conductive spacers. What results is a three dimensional, highly porous and electronically interconnected architecture that is ideal as an electrode structure.

In terms of ORR electrocatalysis, both CNTs[32,33,193,199–201] and graphene-based materials[61,137,138,156] have been shown capable of hosting highly active heteroatom dopant species. In this regard, if the high intrinsic activity of each can be coupled with the benefits of a nanocomposite arrangement, unprecedented performance capabilities may be realized. Lee *et al.*[202] prepared a composite catalyst using the electrostatic interactions between the negative surface charge of GO (prepared by Hummers') and the positive surface charge of CNTs functionalized with PDDA (pCNT). After this self-assembly was facilitated in an aqueous solution containing NaCl, the GO/pCNT assembly was reduced using hydrazine and washed thoroughly. The authors showed that the ratio between GO and the pCNT in the catalyst had an important influence on resulting ORR activity in 0.1 M KOH, and the best performing reduced GO/pCNT composite had an onset potential (−0.23 V *vs.* saturated calomel electrode, SCE) that was 120 and 90 mV higher than that of individual reduced GO and pCNT, respectively. The authors cited an ideal balance between hydrophobic and hydrophilic surface properties that arose due to the composite structure, and contact angle measurements showed an intermediate value between the relatively hydrophilic reduced GO and relatively hydrophobic pCNT. While the authors did not exclusively investigate this, it would be interesting to see if nitrogen dopants are introduced to the structure *via* hydrazine reduction[203,204] and any potential impact they may have on ORR activity.

A hydrothermal approach to develop nitrogen-doped graphene/CNT composites was employed by Chen *et al.*,[205] using ammonia as the reducing and nitrogen doping agent. This was a simple procedure in which GO, oxidized CNTs and ammonia were mixed

together in solution and then transferred to a Teflon-lined autoclave for treated at 180 °C for 12 hours. The authors exclusively showed the beneficial impact on ORR activity of the composite arrangement, which had an onset potential of −0.14 V *vs.* Hg/Hg_2Cl_2 in 0.1 M KOH. On the other hand, N-G and N-CNT prepared by a similar procedure although *in lieu* of the compositing counterpart demonstrated onset potentials of −0.17 and −0.18 V *vs.* Hg/Hg_2Cl_2, respectively. Significantly increased current densities at all potentials were obtained for the N-G/N-CNT composite, and the overall number of electrons transferred was estimated by Koutecky–Levich analysis to range from 3.3 to 3.7 in the −0.4 to −0.7 V *vs.* Hg/Hg_2Cl_2 potential range.

Ratso *et al.*[206] employed a high temperature approach to prepare N-G/N-CNT composites. Hummers' method derived GO was mixed with oxygen functionalized CNTs in the presence of either urea or dicyandiamide, and this mixture was pyrolyzed at 800 °C in argon for 2 hours. For both nitrogen-doped composites, an onset potential of −0.05 V *vs.* SCE towards the ORR was observed in 0.1 M KOH. The N-G/N-CNT derived from dicyandiamide provided much higher activity than that derived from urea, highlighting the importance of appropriate precursor selection during catalyst fabrication. From inspection of the ORR polarization curve, a half-wave potential of the best performing N-G/N-CNT catalyst was −0.26 V *vs.* SCE, and over a 100 mV increase in onset potential in comparison to the undoped G/CNT composite investigated as a comparison.

There are other interesting high temperature methods to prepare N-G/N-CNT composites reported in the literature, such as the growth of CNTs directly on the surface of rGO using chemical vapour deposition. Ma *et al.*[207] impregnated GO with a $NiCl_2$ solution and carried out reduction by the addition of hydrazine. These nickel species then served as catalysts for the chemical vapour deposition of N-CNTs from pyridine vapour, or undoped CNTs using benzene. The nickel species not encapsulated within the graphitic walls of the NCNTs were removed by HCl treatment, however nickel is generally considered inactive towards the ORR. The onset potential in 0.1 M KOH for NCNT/G was −0.191 V *vs.* SCE, a 57 mV improvement over undoped CNT/G. The NCNT/Gs showed an electron transfer number of 3.51 at −0.6 V *vs.* SCE, and that likely increased at even lower electrode potentials as evidenced by the continuously increasing current density. Our group also grew N-CNTs directly on the surface of thermally reduced GO that had been impregnated with ferrocene that acted as a catalyst for CVD growth.[208] The composite catalyst showed a half-wave potential of −0.13 V *vs.* SCE in 0.1 M KOH, however as the growth was catalyzed by an iron-based precursor, this can be considered in the class of M–N–C catalysts discussed in Section 3.1. This brings about an important consideration in that when using carbon nanotubes synthesized in house or purchased from a commercial supplier, one must be careful to verify whether or not they were prepared using iron-based catalysts. The residual iron species have been shown to play an important role in generating ORR activity,[98] and if unaccounted for will surely compromise any claims of "metal-free" ORR catalysis.

We more recently aimed to couple the benefits of dual-doping with those of using graphene/CNT composites.[209] A mixture of GO and oxygen functionalized CNTs were dispersed in acetone for 8 hours in an ultrasonicator kept below 10 °C, followed by evaporation of the solvent under ambient conditions. We then adopted the step-wise doping procedure of Zheng *et al.*[186] to prepare dual-doped sulfur and nitrogen graphene/CNT composite (denoted GC) as depicted in Fig. 16a.[209] In the first step, the GC consisting of CNTs well-dispersed over the surface of GO was partially reduced and nitrogen doped in ammonia at 500 °C. In the second step, the nitrogen-doped GC was mixed with phenyl disulfide and subjected to a heat treatment in argon at 900 °C to form GC-NLS (where L stands for "Low" ammonia treatment temperature). We found that significantly higher nitrogen contents and material yields could be achieved through this step-wise doping approach. Even with a surface concentration of only 0.23 at% sulfur determined by XPS, the beneficial impact on ORR in 0.1 M KOH was substantial. With minimal changes to the GC structure observed after dual-doping (Fig. 16b), the advantages of using this composite arrangement are clearly shown in Fig. 16c. The onset potential of GC-NLS was 0.85 V *vs.* RHE in 0.1 M KOH, a 70 mV improvement over dual-doped graphene (G-NLS) and 50 mV improvement over dual-coped CNTs (C-NLS) prepared by identical procedures. Furthermore, a well-defined mass transport limited current density was achieved and the half-wave potential (0.72 V *vs.* RHE) also represented an increase of 50 and 30 mV, respectively. With the advantages of graphene/CNT nanocomposite structure undebatable, it would be of value to determine exactly what aspects of the structure provide such notable activity improvements. Conducting investigations into optimizing the ratio of GO to CNTs in the initial precursor mixture could also allow for the synergistic effects to be maximized.

As a rarely investigated dopant species, the incorporation of selenium into the structure of a graphene/CNT composite has been previously reported.[210] Commercial GO and CNTs were ultrasonically dispersed in ethanol, followed by the addition of diphenyl diselenide as the dopant precursor. After solvent removal in an evaporating dish, the powder was collected and subjected to a 900 °C heat treatment under argon protection. The authors found a selenide surface content in the composite of 1.05 at% by XPS, and used these results in corroboration with UV-vis to infer that selenium was successfully doped into the graphitic structure of the composite in a selenophene-like form. From ORR activity testing in 0.1 M KOH, all selenide containing structures (Se-CNT, Se-G and Se-CNT/G) outperformed their undoped counterparts. Even more significant was the clear benefit achieved by using this nanocomposite. Over a 100 mV difference was observed between the Se-CNT/G and the next best performing catalyst, Se-CNT. The difference between Se-CNT/G and Se-G was reduced at low overpotentials, but became increasingly more significant at electrode potentials below *ca.* −0.25 V *vs.* Ag/AgCl. Interestingly, while showing promising activity, there exists very little understanding surrounding selenium-doped carbons. This knowledge could be essential for the generation of improved performance ORR electrocatalysts, and it remains to be seen how this species would behave as a co-dopant with nitrogen.

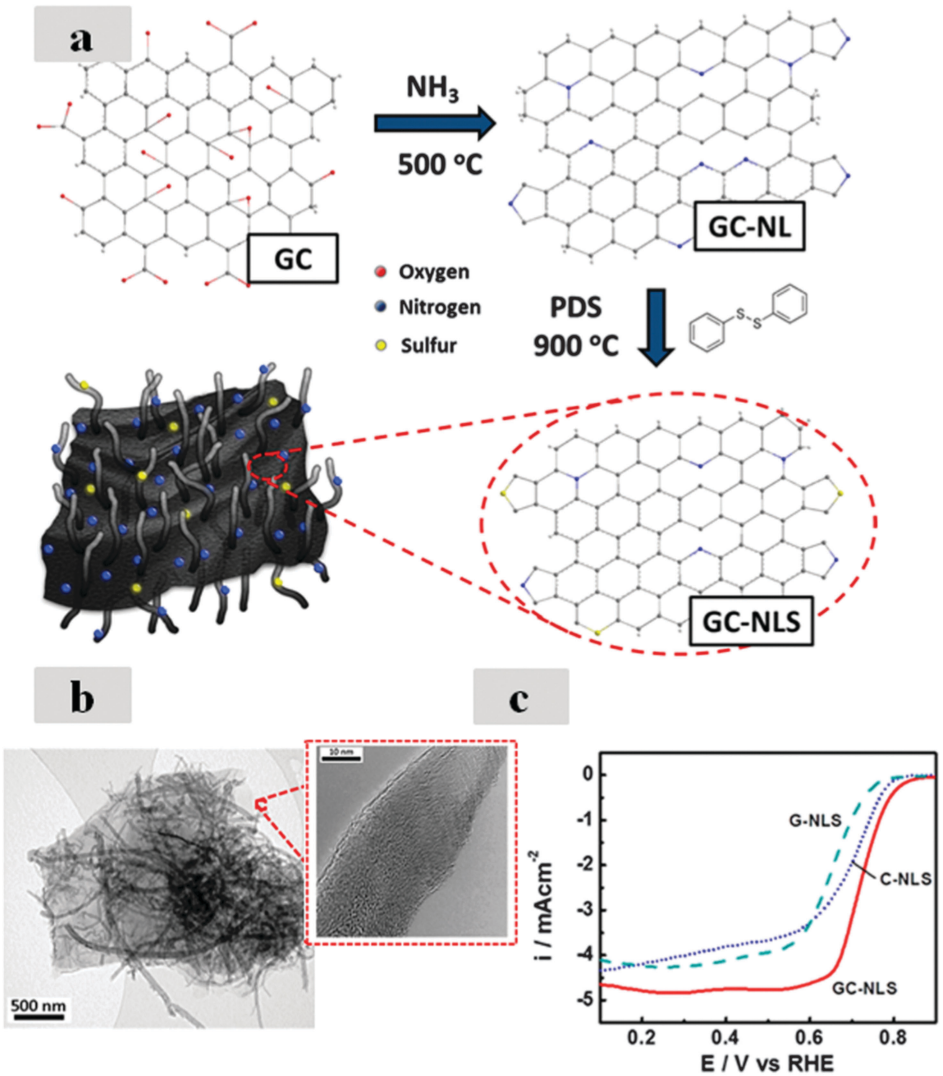

Fig. 16 (a) Schematic of the step-wise doping process to fabricate GC-NLS nanocomposites. (b) TEM images of the GC-NLS catalyst. (c) ORR polarization curves obtained in 0.1 M KOH showing the synergic effect of GC-NLS compared to G-NLS and C-NLS. Reprinted with permission from ref. 209. Copyright (2014) American Chemical Society.

An interesting strategy was taken by Fei *et al.*[211] who used composited zero-dimensional graphene quantum dots (GQDs) with rGO. The GQDs were prepared by subjecting anthracite coal to strongly oxidizing conditions (concentrated H_2SO_4/HNO_3 at 100 °C). They were then dispersed in an aqueous suspension of GO and hydrothermally treated at 140 °C for 14 hours, followed by lyophilisation. The authors opted to use boron and nitrogen as the dual-dopant species, which was accomplished by heat treating the GQD/G composite at 1000 °C in a mixture of boric acid and ammonia vapour. Increasing doping times of 10, 30 and 60 minutes were investigated and found to be directly correlated with increases in the amount of boron and nitrogen doped into the structures. At 30 minutes of doping, the composite structure was found to contain 18.3 at% nitrogen and 13.6 at% boron. This sample showed the highest ORR activity in 0.1 M KOH, whereby it was claimed that at lower doping contents the number of active sites was reduced, whereas at increased contents the formation of directly bonded B–N pairs (*i.e.*, boron nitride) were observed. For the optimal B,N-GQD/G, the ORR production of HO_2^- was less than 4% over the potential range of −0.2 to −0.12 V *vs.* Ag/AgCl (determined using RRDE testing). The onset potential was 0.0 V *vs.* Ag/AgCl, and a visually estimated half-wave potential of −0.21 V *vs.* Ag/AgCl was achieved. The authors showed that individual nitrogen doping of the GQD/G composite was inferior to dual doping, and that using B,N-GQD or B,N-G instead of the composite arrangement also resulted in reduced activity. It was conjectured that, in a case similar to the previously discussed graphene/CNT composites, the advantages of each constituent could be exploited while the drawbacks overcome. In particular, the GQDs provide lots of edge plane exposure that can host ORR active moieties, although their integration into electronically interconnected macrostructures is extremely difficult due to their small size. Graphene thereby

acts as a two-dimensional platform to host uniformly dispersed GQDs, and provides an electronically connective structure that can also host ORR active species.

Zero-dimensional (graphene quantum dots), one-dimensional (CNTs) and two-dimensional (graphene) structures clearly have attractive features that are unique to their structures. By strategically coupling each of these species into composite arrangements, it is expected that very favourable catalyst structures can be formed with a high concentration of active site species. These new designs are worthy of continued investigation as they have the potential to increase catalyst activity and electrode utilization, both through RDE evaluation and in full cells.

5. Conclusions

5.1. Summary

This paper provides a critical review on the important role that graphene and its derivatives have played in ORR electrocatalysis, an important process for PEFC and metal–air battery technologies. As a platinum nanoparticle support, graphene couples a highly graphitic character with excellent surface areas which are attractive features for improving the electrochemical stability and activity of these supported catalysts. The surface chemistry of graphene can also be carefully tuning through either functionalization or heteroatom doping processes. These approaches can be applied to not only aid in the deposition of well distributed, uniformly sized platinum nanoparticles, but also to provide beneficial catalyst support interactions that have been shown capable of providing significant activity and stability improvements. Graphene-based structures have also played an important role in non-precious metal catalysis. Incorporated directly into the reaction mixture or formed *in situ* during pyrolysis induced formation of M–N–C catalysts, the presence of graphene-like structures has been linked to increased electrochemical stability. Furthermore, the two dimensional structure of graphene-based materials and tunable surface has made it attractive as a host to support catalytically active inorganic nanoparticle catalysts that have shown very promising performance in both alkaline and acidic conditions. Finally, graphene-based materials doped with heteroatoms, including nitrogen, sulfur and phosphorus have also been extensively investigated as ORR electrocatalysts, particularly in alkaline conditions. Nitrogen doping has been shown to provide the highest activity towards the ORR, although incorporating nitrogen in tandem with codopants into the structure of graphene-based structures has been shown capable of achieving even further performance enhancements. Different strategies to prepare new graphene-based catalysts are suggested, in addition to clarifying some common misconceptions throughout the literature with recommendations provided on appropriate ORR activity measurement procedures. It is our hope that this consolidated knowledge will serve as a valuable resource for scientists working on developing the next generation of improved performance graphene based catalysts for oxygen reduction.

5.2. Future outlook

Significant progress has been achieved over the past 10 years in understanding the physicochemical properties of graphene. Several notable methods have now been developed to tailor the structure and fine-tune the surface chemistry of these materials. This has already had a notable impact in the field of electrocatalysis, whereby the properties of graphene and its composites have been shown to provide beneficial activity and stability enhancements for the ORR. It is highly expected that with strategically designed research efforts scientists will continue to unlock new potential for the role of graphene in this important area of applied research.

Notwithstanding the great progress, there still remain gaps in fundamental understanding on the exact role of graphene in ORR electrocatalysis. Particularly, further probing how the surface chemistry and physical properties of the graphene influence the resultant activity and stability is desirable. This knowledge can then be applied to achieve unprecendented catalytic performance, allowing scientists to realize the true potential of graphene in electrochemical devices. The approaches and material designs outlined in this review paper provide an excellent starting point for these scientific investigations. Further efforts can apply this as a building block for achieving new fundamental understanding of these materials, along with developing new techniques to carefully design their nanoarchitectures and tailor their surface structures. These approaches should be applied while using sound electrochemical testing practices suggested throughout this review paper, which will allow the community as a whole to situate any newly reported results within the context of the literature.

If the performance of graphene-based catalysts can surpass the performance metrics of conventional systems, high volume production at a low cost will be crucial to achieving commercial success. High production manufacturing is not an issue considered in depth throughout this review paper; however it is important that readers are aware of this long term implication. In fact, great progress has been realized in recent years towards scaling up the production quantities of graphene and its derivatives. Researchers and industry must team up to translate this success towards the best performing graphene-based ORR electrocatalysts. Only then can these materials be integrated into practical devices for widespread application.

List of acronyms

AEI	Anion exchange ionomer
AEM	Alkaline exchange membrane
Ag/AgCl	Silver/silver chloride reference electrode
BET	Brunauer–Emmett–Teller
CV	Cyclic voltammetry
CNT	Carbon nanotube
DFT	Density functional theory
ECSA	Electrochemical surface area
EDA	Ethylenediamine
Fe-Pc	Iron phthalocyanine

GQD	Graphene quantum dot
GO	Graphene oxide
HRTEM	High resolution transmission electron microscopy
ICP	Inductively coupled plasma
IL	Ionic liquid
LSV	Linear sweep voltammetry
MEA	Membrane electrode assembly
MMT	Montmorillonite
M–N–C	Transition metal–nitrogen–carbon complexes
MOF	Metal organic framework
MWNT	Multi-walled carbon nanotubes
N-CNT	Nitrogen-doped CNT
NG	Nitrogen-doped graphene-based materials
non-PGM	Non-platinum group metal
NPMC	Non-precious metal catalyst
ORR	Oxygen reduction reaction
PANI	Polyaniline
PDDA	Poly(diallyldimethylammonium chloride)
PEFC	Polymer electrolyte fuel cell
Pt/C	Conventional carbon black supported platinum
PtNT	Platinum nanotube
PtNW	Platinum nanowire
RDE	Rotating disk electrode
rGO	Reduced graphene oxide
RHE	Reversible hydrogen electrode
RRDE	Rotating ring disk electrode
SCE	Saturated calomel electrode
SEM	Scanning electron microscopy
SG	Sulfur-doped graphene-based materials
TEM	Transmission electron microscopy
XANES	X-ray absorption near-edge structure
XPS	X-ray photoelectron spectroscopy
ZIF	Zeolitic imidazolate frameworks

References

1 E. Bi, H. Chen, X. Yang, W. Peng, M. Grätzel and L. Han, A quasi core–shell nitrogen-doped graphene/cobalt sulfide conductive catalyst for highly efficient dye-sensitized solar cells, *Energy Environ. Sci.*, 2014, **7**, 2637.

2 Y. Jiao, Y. Zheng, M. Jaroniec and S. Z. Qiao, Origin of the electrocatalytic oxygen reduction activity of graphene-based catalysts: a roadmap to achieve the best performance, *J. Am. Chem. Soc.*, 2014, **136**, 4394–4403.

3 U.S. Drive, Fuel Cell Technical Team Roadmap, 2013. Available online at: http://energy.gov/sites/prod/files/2014/02/f8/fctt_roadmap_june2013.pdf.

4 U. Eberle, B. Muller and R. von Helmolt, Fuel cell electric vehicles and hydrogen infrastructure: status, *Energy Environ. Sci.*, 2012, **5**, 8780–8798.

5 B. Huskinson, M. P. Marshak, C. Suh, S. Er, M. R. Gerhardt, C. J. Galvin, X. Chen, A. Aspuru-Guzik, R. G. Gordon and M. J. Aziz, A metal-free organic-inorganic aqueous flow battery, *Nature*, 2014, **505**, 195–198.

6 K. Lin, Q. Chen, M. R. Gerhardt, L. Tong, S. B. Kim, L. Eisenach, A. W. Valle, D. Hardee, R. G. Gordon, M. J. Aziz and M. P. Marshak, Alkaline quinone flow battery, *Science*, 2015, **349**, 1529–1532.

7 A. Weber, M. Mench, J. Meyers, P. Ross, J. Gostick and Q. Liu, Redox flow batteries: a review, *J. Appl. Electrochem.*, 2011, **41**, 1137–1164.

8 B. Dunn, H. Kamath and J.-M. Tarascon, Electrical Energy Storage for the Grid: A Battery of Choices, *Science*, 2011, **334**, 928–935.

9 J. Ozaki, S. Tanifuji, A. Furuichi and K. Yabutsuka, Enhancement of oxygen reduction activity of nanoshell carbons by introducing nitrogen atoms from metal phthalocyanines, *Electrochim. Acta*, 2010, **55**, 1864–1871.

10 F. Cheng and J. Chen, metal–air batteries: from oxygen reduction electrochemistry to cathode catalysts, *Chem. Soc. Rev.*, 2012, **41**, 2172–2192.

11 J. Wu and H. Yang, Platinum-Based Oxygen Reduction Electrocatalysts, *Acc. Chem. Res.*, 2013, **46**, 1848–1857.

12 D. C. Higgins and Z. Chen, Recent progress in non-precious metal catalysts for PEM fuel cell applications, *Can. J. Chem. Eng.*, 2013, **91**, 1881–1895.

13 Z. Chen, D. Higgins, A. Yu, L. Zhang and J. Zhang, A review on non-precious metal electrocatalysts for PEM fuel cells, *Energy Environ. Sci.*, 2011, **4**, 3167–3192.

14 F. Jaouen, E. Proietti, M. Lefèvre, R. Chenitz, J.-P. Dodelet, G. Wu, H. T. Chung, C. M. Johnston and P. Zelenay, Recent advances in non-precious metal catalysis for oxygen-reduction reaction in polymer electrolyte fuel cells, *Energy Environ. Sci.*, 2011, **4**, 114.

15 J. Wu, X. Z. Yuan, J. J. Martin, H. Wang, J. Zhang, J. Shen, S. Wu and W. Merida, A review of PEM fuel cell durability: degradation mechanisms and mitigation strategies, *J. Power Sources*, 2008, **184**, 104–119.

16 T. Kinumoto, M. Inaba, Y. Nakayama, K. Ogata, R. Umebayashi, A. Tasaka, Y. Iriyama, T. Abe and Z. Ogumi, Durability of perfluorinated ionomer membrane against hydrogen peroxide, *J. Power Sources*, 2006, **158**, 1222–1228.

17 R. Borup, J. Meyers, B. Pivovar, Y. S. Kim, R. Mukundan, N. Garland, D. Myers, M. Wilson, F. Garzon, D. Wood, P. Zelenay, K. More, K. Stroh, T. Zawodzinski, J. Boncella, J. E. McGrath, M. Inaba, K. Miyatake, M. Hori, K. Ota, Z. Ogumi, S. Miyata, A. Nishikata, Z. Siroma, Y. Uchimoto, K. Yasuda, K.-i. Kimijima and N. Iwashita, Scientific Aspects of Polymer Electrolyte Fuel Cell Durability and Degradation, *Chem. Rev.*, 2007, **107**, 3904–3951.

18 M. K. Debe, Electrocatalyst approaches and challenges for automotive fuel cells, *Nature*, 2012, **486**, 43–51.

19 D. Higgins, M. A. Hoque, M. H. Seo, R. Wang, F. Hassan, J.-Y. Choi, M. Pritzker, A. Yu, J. Zhang and Z. Chen, Development and Simulation of Sulfur-doped Graphene Supported Platinum with Exemplary Stability and Activity Towards Oxygen Reduction, *Adv. Funct. Mater.*, 2014, **24**, 4325–4336.

20 M. A. Hoque, F. M. Hassan, D. Higgins, J.-Y. Choi, M. Pritzker, S. Knights, S. Ye and Z. Chen, Multigrain

Platinum Nanowires Consisting of Oriented Nanoparticles Anchored on Sulfur-Doped Graphene as a Highly Active and Durable Oxygen Reduction Electrocatalyst, *Adv. Mater.*, 2015, **27**, 1229–1234.

21 Y. Tan, C. Xu, G. Chen, N. Zheng and Q. Xie, A graphene-platinum nanoparticles-ionic liquid composite catalyst for methanol-tolerant oxygen reduction reaction, *Energy Environ. Sci.*, 2012, **5**, 6923–6927.

22 J. Zhu, M. Xiao, X. Zhao, C. Liu, J. Ge and W. Xing, Strongly coupled Pt nanotubes/N-doped graphene as highly active and durable electrocatalysts for oxygen reduction reaction, *Nano Energy*, 2015, **13**, 318–326.

23 G. Wu and P. Zelenay, Nanostructured Nonprecious Metal Catalysts for Oxygen Reduction Reaction, *Acc. Chem. Res.*, 2013, **46**, 1878–1889.

24 V. Chabot, D. Higgins, A. Yu, X. Xiao, Z. Chen and J. Zhang, A review of graphene and graphene oxide sponge: material synthesis and applications to energy and the environment, *Energy Environ. Sci.*, 2014, **7**, 1564–1596.

25 X. Zhou, J. Qiao, L. Yang and J. Zhang, A Review of Graphene-Based Nanostructural Materials for Both Catalyst Supports and Metal-Free Catalysts in PEM Fuel Cell Oxygen Reduction Reactions, *Adv. Energy Mater.*, 2014, **4**, 1301523.

26 H. Peng, Z. Mo, S. Liao, H. Liang, L. Yang, F. Luo, H. Song, Y. Zhong and B. Zhang, High Performance Fe- and N-Doped Carbon Catalyst with Graphene Structure for Oxygen Reduction, *Sci. Rep.*, 2013, **3**, 1765.

27 A. Serov, K. Artyushkova and P. Atanassov, Fe–N–C Oxygen Reduction Fuel Cell Catalyst Derived from Carbendazim: Synthesis, Structure, and Reactivity, *Adv. Energy Mater.*, 2014, **4**, 1301735.

28 G. K. H. Wiberg, K. J. J. Mayrhofer and M. Arenz, Investigation of the Oxygen Reduction Activity on Silver – A Rotating Disc Electrode Study, *Fuel Cells*, 2010, **10**, 575–581.

29 R. Cao, J.-S. Lee, M. Liu and J. Cho, Recent Progress in Non-Precious Catalysts for metal–air Batteries, *Adv. Energy Mater.*, 2012, **2**, 816–829.

30 Y. Gorlin and T. F. Jaramillo, A Bifunctional Nonprecious Metal Catalyst for Oxygen Reduction and Water Oxidation, *J. Am. Chem. Soc.*, 2010, **132**, 13612–13614.

31 Y. Gorlin, C.-J. Chung, D. Nordlund, B. M. Clemens and T. F. Jaramillo, Mn_3O_4 Supported on Glassy Carbon: An Active Non-Precious Metal Catalyst for the Oxygen Reduction Reaction, *ACS Catal.*, 2012, **2**, 2687–2694.

32 K. Gong, F. Du, Z. Xia, M. Durstock and L. Dai, Nitrogen-Doped Carbon Nanotube Arrays with High Electrocatalytic Activity for Oxygen Reduction, *Science*, 2009, **323**, 760–764.

33 Z. Chen, D. Higgins and Z. Chen, Nitrogen doped carbon nanotubes and their impact on the oxygen reduction reaction in fuel cells, *Carbon*, 2010, **48**, 3057–3065.

34 S. Chen, J. Bi, Y. Zhao, L. Yang, C. Zhang, Y. Ma, Q. Wu, X. Wang and Z. Hu, Nitrogen-Doped Carbon Nanocages as Efficient Metal-Free Electrocatalysts for Oxygen Reduction Reaction, *Adv. Mater.*, 2012, **24**, 5593–5597.

35 Q. Li, R. Cao, J. Cho and G. Wu, Nanocarbon Electrocatalysts for Oxygen Reduction in Alkaline Media for Advanced Energy Conversion and Storage, *Adv. Energy Mater.*, 2014, **4**, 1301415.

36 M. Liu, R. Zhang and W. Chen, Graphene-Supported Nanoelectrocatalysts for Fuel Cells: Synthesis, Properties, and Applications, *Chem. Rev.*, 2014, **114**, 5117–5160.

37 K. S. Novoselov, A. K. Geim, S. V. Morozov, D. Jiang, Y. Zhang, S. V. Dubonos, I. V. Grigorieva and A. A. Firsov, Electric Field Effect in Atomically Thin Carbon Films, *Science*, 2004, **306**, 666–669.

38 A. K. Geim and K. S. Novoselov, The rise of graphene, *Nat. Mater.*, 2007, **6**, 183–191.

39 M. J. Allen, V. C. Tung and R. B. Kaner, Honeycomb Carbon: A Review of Graphene, *Chem. Rev.*, 2010, **110**, 132–145.

40 A. Bianco, H.-M. Cheng, T. Enoki, Y. Gogotsi, R. H. Hurt, N. Koratkar, T. Kyotani, M. Monthioux, C. R. Park, J. M. D. Tascon and J. Zhang, All in the graphene family – A recommended nomenclature for two-dimensional carbon materials, *Carbon*, 2013, **65**, 1–6.

41 H. Wang, T. Maiyalagan and X. Wang, Review on Recent Progress in Nitrogen-Doped Graphene: Synthesis, Characterization, and Its Potential Applications, *ACS Catal.*, 2012, **2**, 781–794.

42 W. Choi, I. Lahiri, R. Seelaboyina and Y. S. Kang, Synthesis of Graphene and Its Applications: A Review, *Crit. Rev. Solid State Mater. Sci.*, 2010, **35**, 52–71.

43 A. K. Geim, Graphene: Status and Prospects, *Science*, 2009, **324**, 1530–1534.

44 W. S. Hummers and R. E. Offeman, Preparation of Graphitic Oxide, *J. Am. Chem. Soc.*, 1958, **80**, 1339.

45 Z.-H. Sheng, L. Shao, J.-J. Chen, W.-J. Bao, F.-B. Wang and X.-H. Xia, Catalyst-Free Synthesis of Nitrogen-Doped Graphene *via* Thermal Annealing Graphite Oxide with Melamine and Its Excellent Electrocatalysis, *ACS Nano*, 2011, **5**, 4350–4358.

46 S. Stankovich, D. A. Dikin, R. D. Piner, K. A. Kohlhaas, A. Kleinhammes, Y. Jia, Y. Wu, S. T. Nguyen and R. S. Ruoff, Synthesis of graphene-based nanosheets *via* chemical reduction of exfoliated graphite oxide, *Carbon*, 2007, **45**, 1558–1565.

47 C. Nethravathi and M. Rajamathi, Chemically modified graphene sheets produced by the solvothermal reduction of colloidal dispersions of graphite oxide, *Carbon*, 2008, **46**, 1994–1998.

48 W. Gao, L. B. Alemany, L. Ci and P. M. Ajayan, New insights into the structure and reduction of graphite oxide, *Nat. Chem.*, 2009, **1**, 403–408.

49 Z. Chen, A. Yu, D. Higgins, H. Li, H. Wang and Z. Chen, Highly Active and Durable Core–Corona Structured Bifunctional Catalyst for Rechargeable Metal–Air Battery Application, *Nano Lett.*, 2012, **12**, 1946–1952.

50 D. C. Higgins, D. Meza and Z. Chen, Nitrogen-Doped Carbon Nanotubes as Platinum Catalyst Supports for Oxygen Reduction Reaction in Proton Exchange Membrane Fuel Cells, *J. Phys. Chem. C*, 2010, **114**, 21982–21988.

51 Y. Shao, S. Zhang, C. Wang, Z. Nie, J. Liu, Y. Wang and Y. Lin, Highly durable graphene nanoplatelets supported

Pt nanocatalysts for oxygen reduction, *J. Power Sources*, 2010, **195**, 4600–4605.
52 W. He, H. Jiang, Y. Zhou, S. Yang, X. Xue, Z. Zou, X. Zhang, D. L. Akins and H. Yang, An efficient reduction route for the production of Pd–Pt nanoparticles anchored on graphene nanosheets for use as durable oxygen reduction electrocatalysts, *Carbon*, 2012, **50**, 265–274.
53 L. Zeng, T. S. Zhao, L. An, G. Zhao, X. H. Yan and C. Y. Jung, Graphene-supported platinum catalyst prepared with ionomer as surfactant for anion exchange membrane fuel cells, *J. Power Sources*, 2015, **275**, 506–515.
54 D. He, K. Cheng, H. Li, T. Peng, F. Xu, S. Mu and M. Pan, Highly Active Platinum Nanoparticles on Graphene Nanosheets with a Significant Improvement in Stability and CO Tolerance, *Langmuir*, 2012, **28**, 3979–3986.
55 J. I. Paredes, S. Villar-Rodil, A. Martínez-Alonso and J. M. D. Tascón, Graphene Oxide Dispersions in Organic Solvents, *Langmuir*, 2008, **24**, 10560–10564.
56 D. R. Dreyer, S. Park, C. W. Bielawski and R. S. Ruoff, The chemistry of graphene oxide, *Chem. Soc. Rev.*, 2010, **39**, 228–240.
57 B. Seger and P. V. Kamat, Electrocatalytically Active Graphene-Platinum Nanocomposites. Role of 2-D Carbon Support in PEM Fuel Cells, *J. Phys. Chem. C*, 2009, **113**, 7990–7995.
58 H.-W. Ha, I. Y. Kim, S.-J. Hwang and R. S. Ruoff, One-Pot Synthesis of Platinum Nanoparticles Embedded on Reduced Graphene Oxide for Oxygen Reduction in Methanol Fuel Cells, *Electrochem. Solid-State Lett.*, 2011, **14**, B70.
59 K. Zhang, Q. Yue, G. Chen, Y. Zhai, L. Wang, H. Wang, J. Zhao, J. Liu, J. Jia and H. Li, Effects of Acid Treatment of Pt–Ni Alloy Nanoparticles@Graphene on the Kinetics of the Oxygen Reduction Reaction in Acidic and Alkaline Solutions, *J. Phys. Chem. C*, 2011, **115**, 379–389.
60 D. Chen, X. Zhao, S. Chen, H. Li, X. Fu, Q. Wu, S. Li, Y. Li, B.-L. Su and R. S. Ruoff, One-pot fabrication of FePt/reduced graphene oxide composites as highly active and stable electrocatalysts for the oxygen reduction reaction, *Carbon*, 2014, **68**, 755–762.
61 D. U. Lee, H. W. Park, D. Higgins, L. Nazar and Z. Chen, Highly Active Graphene Nanosheets Prepared *via* Extremely Rapid Heating as Efficient Zinc-Air Battery Electrode Material, *J. Electrochem. Soc.*, 2013, **160**, F910–F915.
62 R. Kou, Y. Shao, D. Wang, M. H. Engelhard, J. H. Kwak, J. Wang, V. V. Viswanathan, C. Wang, Y. Lin, Y. Wang, I. A. Aksay and J. Liu, Enhanced activity and stability of Pt catalysts on functionalized graphene sheets for electrocatalytic oxygen reduction, *Electrochem. Commun.*, 2009, **11**, 954–957.
63 M. H. Seo, S. M. Choi, H. J. Kim and W. B. Kim, The graphene-supported Pd and Pt catalysts for highly active oxygen reduction reaction in an alkaline condition, *Electrochem. Commun.*, 2011, **13**, 182–185.
64 J. Snyder, T. Fujita, M. W. Chen and J. Erlebacher, Oxygen reduction in nanoporous metal-ionic liquid composite electrocatalysts, *Nat. Mater.*, 2010, **9**, 904–907.
65 M. Shao, A. Peles and K. Shoemaker, Electrocatalysis on Platinum Nanoparticles: Particle Size Effect on Oxygen Reduction Reaction Activity, *Nano Lett.*, 2011, **11**, 3714–3719.
66 K. Kinoshita, Particle Size Effects for Oxygen Reduction on Highly Dispersed Platinum in Acid Electrolytes, *J. Electrochem. Soc.*, 1990, **137**, 845–848.
67 S. Guo and S. Sun, FePt nanoparticles assembled on graphene as enhanced catalyst for oxygen reduction reaction, *J. Am. Chem. Soc.*, 2012, **134**, 2492–2495.
68 Y. Si and E. T. Samulski, Exfoliated Graphene Separated by Platinum Nanoparticles, *Chem. Mater.*, 2008, **20**, 6792–6797.
69 Y. Xin, J.-g. Liu, Y. Zhou, W. Liu, J. Gao, Y. Xie, Y. Yin and Z. Zou, Preparation and characterization of Pt supported on graphene with enhanced electrocatalytic activity in fuel cell, *J. Power Sources*, 2011, **196**, 1012–1018.
70 Y. Li, Y. Li, E. Zhu, T. McLouth, C. Y. Chiu, X. Huang and Y. Huang, Stabilization of high-performance oxygen reduction reaction Pt electrocatalyst supported on reduced graphene oxide/carbon black composite, *J. Am. Chem. Soc.*, 2012, **134**, 12326–12329.
71 S. S. Jyothirmayee Aravind, R. Imran Jafri, N. Rajalakshmi and S. Ramaprabhu, Solar exfoliated graphene-carbon nanotube hybrid nano composites as efficient catalyst supports for proton exchange membrane fuel cells, *J. Mater. Chem.*, 2011, **21**, 18199–18204.
72 Y. Zhou, K. Neyerlin, T. S. Olson, S. Pylypenko, J. Bult, H. N. Dinh, T. Gennett, Z. Shao and R. O'Hayre, Enhancement of Pt and Pt-alloy fuel cell catalyst activity and durability *via* nitrogen-modified carbon supports, *Energy Environ. Sci.*, 2010, **3**, 1437–1446.
73 Y. Chen, J. Wang, H. Liu, M. N. Banis, R. Li, X. Sun, T.-K. Sham, S. Ye and S. Knights, Nitrogen Doping Effects on Carbon Nanotubes and the Origin of the Enhanced Electrocatalytic Activity of Supported Pt for Proton-Exchange Membrane Fuel Cells, *J. Phys. Chem. C*, 2011, **115**, 3769–3776.
74 Y. Chen, J. Wang, H. Liu, R. Li, X. Sun, S. Ye and S. Knights, Enhanced stability of Pt electrocatalysts by nitrogen doping in CNTs for PEM fuel cells, *Electrochem. Commun.*, 2009, **11**, 2071–2076.
75 M. S. Saha, R. Li, X. Sun and S. Ye, 3-D composite electrodes for high performance PEM fuel cells composed of Pt supported on nitrogen-doped carbon nanotubes grown on carbon paper, *Electrochem. Commun.*, 2009, **11**, 438–441.
76 G. Vijayaraghavan and K. J. Stevenson, Synergistic Assembly of Dendrimer-Templated Platinum Catalysts on Nitrogen-Doped Carbon Nanotube Electrodes for Oxygen Reduction, *Langmuir*, 2007, **23**, 5279–5282.
77 J. Bai, Q. Zhu, Z. Lv, H. Dong, J. Yu and L. Dong, Nitrogen-doped graphene as catalysts and catalyst supports for oxygen reduction in both acidic and alkaline solutions, *Int. J. Hydrogen Energy*, 2013, **38**, 1413–1418.
78 D. He, Y. Jiang, H. Lv, M. Pan and S. Mu, Nitrogen-doped reduced graphene oxide supports for noble metal catalysts with greatly enhanced activity and stability, *Appl. Catal., B*, 2013, **132–133**, 379–388.

79 D. He, K. Cheng, T. Peng, X. Sun, M. Pan and S. Mu, Bifunctional effect of reduced graphene oxides to support active metal nanoparticles for oxygen reduction reaction and stability, *J. Mater. Chem.*, 2012, **22**, 21298–21304.
80 R. Imran Jafri, N. Rajalakshmi and S. Ramaprabhu, Nitrogen doped graphene nanoplatelets as catalyst support for oxygen reduction reaction in proton exchange membrane fuel cell, *J. Mater. Chem.*, 2010, **20**, 7114.
81 B. P. Vinayan, R. Nagar, N. Rajalakshmi and S. Ramaprabhu, Novel Platinum–Cobalt Alloy Nanoparticles Dispersed on Nitrogen-Doped Graphene as a Cathode Electrocatalyst for PEMFC Applications, *Adv. Funct. Mater.*, 2012, **22**, 3519–3526.
82 B. P. Vinayan and S. Ramaprabhu, Platinum-TM (TM = Fe, Co) alloy nanoparticles dispersed nitrogen doped (reduced graphene oxide-multiwalled carbon nanotube) hybrid structure cathode electrocatalysts for high performance PEMFC applications, *Nanoscale*, 2013, **5**, 5109–5118.
83 Z. Chen, M. Waje, W. Li and Y. Yan, Supportless Pt and PtPd Nanotubes as Electrocatalysts for Oxygen-Reduction Reactions, *Angew. Chem., Int. Ed.*, 2007, **46**, 4060–4063.
84 D. C. Higgins, R. Wang, M. A. Hoque, P. Zamani, S. Abureden and Z. Chen, Morphology and composition controlled platinum–cobalt alloy nanowires prepared by electrospinning as oxygen reduction catalyst, *Nano Energy*, 2014, **10**, 135–143.
85 C. Koenigsmann, W.-P. Zhou, R. R. Adzic, E. Sutter and S. S. Wong, Size-Dependent Enhancement of Electrocatalytic Performance in Relatively Defect-Free, Processed Ultrathin Platinum Nanowires, *Nano Lett.*, 2010, **10**, 2806–2811.
86 X. Ji, K. T. Lee, R. Holden, L. Zhang, J. Zhang, G. A. Botton, M. Couillard and L. F. Nazar, Nanocrystalline intermetallics on mesoporous carbon for direct formic acid fuel cell anodes, *Nat. Chem.*, 2010, **2**, 286–293.
87 R. Wang, D. C. Higgins, M. A. Hoque, D. Lee, F. Hassan and Z. Chen, Controlled growth of platinum nanowire arrays on sulfur doped graphene as high performance electrocatalyst, *Sci. Rep.*, 2013, **3**, 2431.
88 D. C. Higgins, S. Ye, S. Knights and Z. Chen, Highly Durable Platinum-Cobalt Nanowires by Microwave Irradiation as Oxygen Reduction Catalyst for PEM Fuel Cell, *Electrochem. Solid-State Lett.*, 2012, **15**, B83–B85.
89 G. Wu and P. Zelenay, Nanostructured Nonprecious Metal Catalysts for Oxygen Reduction Reaction, *Acc. Chem. Res.*, 2013, **46**, 1878–1889.
90 M. A. Rahman, X. Wang and C. Wen, High Energy Density metal–air Batteries: A Review, *J. Electrochem. Soc.*, 2013, **160**, A1759–A1771.
91 D. Zhao, J. L. Shui, L. R. Grabstanowicz, C. Chen, S. M. Commet, T. Xu, J. Lu and D. J. Liu, Highly efficient non-precious metal electrocatalysts prepared from one-pot synthesized zeolitic imidazolate frameworks, *Adv. Mater.*, 2014, **26**, 1093–1097.
92 A. Serov, K. Artyushkova, N. I. Andersen, S. Stariha and P. Atanassov, Original Mechanochemical Synthesis of Non-Platinum Group Metals Oxygen Reduction Reaction Catalysts Assisted by Sacrificial Support Method, *Electrochim. Acta*, 2015, **179**, 154–160.
93 A. Serov, M. H. Robson, M. Smolnik and P. Atanassov, Tri-metallic transition metal–nitrogen–carbon catalysts derived by sacrificial support method synthesis, *Electrochim. Acta*, 2013, **109**, 433–439.
94 U. Tylus, Q. Jia, K. Strickland, N. Ramaswamy, A. Serov, P. Atanassov and S. Mukerjee, Elucidating Oxygen Reduction Active Sites in Pyrolyzed Metal–Nitrogen Coordinated Non-Precious-Metal Electrocatalyst Systems, *J. Phys. Chem. C*, 2014, **118**, 8999–9008.
95 G. Wu, K. L. More, C. M. Johnston and P. Zelenay, High-Performance Electrocatalysts for Oxygen Reduction Derived from Polyaniline, Iron, and Cobalt, *Science*, 2011, **332**, 443–447.
96 G. Wu, C. M. Johnston, N. H. Mack, K. Artyushkova, M. Ferrandon, M. Nelson, J. S. Lezama-Pacheco, S. D. Conradson, K. L. More, D. J. Myers and P. Zelenay, Synthesis–structure–performance correlation for polyaniline–Me–C non-precious metal cathode catalysts for oxygen reduction in fuel cells, *J. Mater. Chem.*, 2011, **21**, 11392.
97 G. Wu, K. L. More, P. Xu, H. L. Wang, M. Ferrandon, A. J. Kropf, D. J. Myers, S. Ma, C. M. Johnston and P. Zelenay, A carbon-nanotube-supported graphene-rich non-precious metal oxygen reduction catalyst with enhanced performance durability, *Chem. Commun.*, 2013, **49**, 3291–3293.
98 Y. Li, W. Zhou, H. Wang, L. Xie, Y. Liang, F. Wei, J. C. Idrobo, S. J. Pennycook and H. Dai, An oxygen reduction electrocatalyst based on carbon nanotube-graphene complexes, *Nat. Nanotechnol.*, 2012, **7**, 394–400.
99 W. Ma, P. Yu, T. Ohsaka and L. Mao, An efficient electrocatalyst for oxygen reduction reaction derived from a Co-porphyrin-based covalent organic framework, *Electrochem. Commun.*, 2015, **52**, 53–57.
100 Q. Li, P. Xu, W. Gao, S. Ma, G. Zhang, R. Cao, J. Cho, H. L. Wang and G. Wu, Graphene/graphene-tube nanocomposites templated from cage-containing metal-organic frameworks for oxygen reduction in Li-O(2) batteries, *Adv. Mater.*, 2014, **26**, 1378–1386.
101 K. Strickland, E. Miner, Q. Jia, U. Tylus, N. Ramaswamy, W. Liang, M. T. Sougrati, F. Jaouen and S. Mukerjee, Highly active oxygen reduction non-platinum group metal electrocatalyst without direct metal-nitrogen coordination, *Nat. Commun.*, 2015, **6**, 7343.
102 K. Parvez, S. Yang, Y. Hernandez, A. Winter, A. Turchanin, X. Feng and K. Müllen, Nitrogen-Doped Graphene and Its Iron-Based Composite As Efficient Electrocatalysts for Oxygen Reduction Reaction, *ACS Nano*, 2012, **6**, 9541–9550.
103 H. R. Byon, J. Suntivich and Y. Shao-Horn, Graphene-Based Non-Noble-Metal Catalysts for Oxygen Reduction Reaction in Acid, *Chem. Mater.*, 2011, **23**, 3421–3428.
104 H. Yin, C. Zhang, F. Liu and Y. Hou, Hybrid of Iron Nitride and Nitrogen-Doped Graphene Aerogel as Synergistic Catalyst for Oxygen Reduction Reaction, *Adv. Funct. Mater.*, 2014, **24**, 2930–2937.

105 W. Bian, Z. Yang, P. Strasser and R. Yang, A $CoFe_2O_4$/graphene nanohybrid as an efficient bi-functional electrocatalyst for oxygen reduction and oxygen evolution, *J. Power Sources*, 2014, **250**, 196–203.

106 C. H. Choi, M. W. Chung, H. C. Kwon, J. H. Chung and S. I. Woo, Nitrogen-doped graphene/carbon nanotube self-assembly for efficient oxygen reduction reaction in acid media, *Appl. Catal., B*, 2014, **144**, 760–766.

107 C. H. Choi, H. K. Lim, M. W. Chung, J. C. Park, H. Shin, H. Kim and S. I. Woo, Long-range electron transfer over graphene-based catalyst for high-performing oxygen reduction reactions: importance of size, N-doping, and metallic impurities, *J. Am. Chem. Soc.*, 2014, **136**, 9070–9077.

108 X. Fu, Y. Liu, X. Cao, J. Jin, Q. Liu and J. Zhang, $FeCo–N_x$ embedded graphene as high performance catalysts for oxygen reduction reaction, *Appl. Catal., B*, 2013, **130–131**, 143–151.

109 K. Kamiya, K. Hashimoto and S. Nakanishi, Instantaneous one-pot synthesis of Fe-N-modified graphene as an efficient electrocatalyst for the oxygen reduction reaction in acidic solutions, *Chem. Commun.*, 2012, **48**, 10213–10215.

110 S. Zhang, H. Zhang, Q. Liu and S. Chen, Fe–N doped carbon nanotube/graphene composite: facile synthesis and superior electrocatalytic activity, *J. Mater. Chem. A*, 2013, **1**, 3302.

111 H. X. Zhong, J. Wang, Y. W. Zhang, W. L. Xu, W. Xing, D. Xu, Y. F. Zhang and X. B. Zhang, ZIF-8 derived graphene-based nitrogen-doped porous carbon sheets as highly efficient and durable oxygen reduction electrocatalysts, *Angew. Chem., Int. Ed.*, 2014, **53**, 14235–14239.

112 Z. Chen, D. Higgins, H. Tao, R. S. Hsu and Z. Chen, Highly Active Nitrogen-Doped Carbon Nanotubes for Oxygen Reduction Reaction in Fuel Cell Applications, *J. Phys. Chem.*, 2009, **113**, 21008–21013.

113 H. T. Chung, J. H. Won and P. Zelenay, Active and stable carbon nanotube/nanoparticle composite electrocatalyst for oxygen reduction, *Nat. Commun.*, 2013, **4**, 1922.

114 K. Parvez, S. Yang, Y. Hernandez, A. Winter, A. Turchanin, X. Feng and K. Müllen, Nitrogen-Doped Graphene and Its Iron-Based Composite As Efficient Electrocatalysts for Oxygen Reduction Reaction, *ACS Nano*, 2012, **6**, 9541–9550.

115 Y. Jiang, Y. Lu, X. Lv, D. Han, Q. Zhang, L. Niu and W. Chen, Enhanced Catalytic Performance of Pt-Free Iron Phthalocyanine by Graphene Support for Efficient Oxygen Reduction Reaction, *ACS Catal.*, 2013, **3**, 1263–1271.

116 T. Li, Y. Peng, K. Li, R. Zhang, L. Zheng, D. Xia and X. Zuo, Enhanced activity and stability of binuclear iron(III) phthalocyanine on graphene nanosheets for electrocatalytic oxygen reduction in acid, *J. Power Sources*, 2015, **293**, 511–518.

117 C. Zhang, R. Hao, H. Yin, F. Liu and Y. Hou, Iron phthalocyanine and nitrogen-doped graphene composite as a novel non-precious catalyst for the oxygen reduction reaction, *Nanoscale*, 2012, **4**, 7326–7329.

118 M. R. Gao, Y. F. Xu, J. Jiang and S. H. Yu, Nanostructured metal chalcogenides: synthesis, modification, and applications in energy conversion and storage devices, *Chem. Soc. Rev.*, 2013, **42**, 2986–3017.

119 H. Wang, Y. Liang, Y. Li and H. Dai, $Co_{(1-x)}S$-graphene hybrid: a high-performance metal chalcogenide electrocatalyst for oxygen reduction, *Angew. Chem., Int. Ed.*, 2011, **50**, 10969–10972.

120 D. C. Higgins, F. M. Hassan, M. H. Seo, J. Y. Choi, M. A. Hoque, D. U. Lee and Z. Chen, Shape-controlled octahedral cobalt disulfide nanoparticles supported on nitrogen and sulfur-doped graphene/carbon nanotube composites for oxygen reduction in acidic electrolyte, *J. Mater. Chem. A*, 2015, **3**, 6340–6350.

121 J. Duan, Y. Zheng, S. Chen, Y. Tang, M. Jaroniec and S. Qiao, Mesoporous hybrid material composed of Mn_3O_4 nanoparticles on nitrogen-doped graphene for highly efficient oxygen reduction reaction, *Chem. Commun.*, 2013, **49**, 7705–7707.

122 N. Mahmood, C. Zhang, J. Jiang, F. Liu and Y. Hou, Multifunctional Co_3S_4/graphene composites for lithium ion batteries and oxygen reduction reaction, *Chem. – Eur. J.*, 2013, **19**, 5183–5190.

123 Q. Liu, J. Jin and J. Zhang, $NiCo_2S_4$@graphene as a bifunctional electrocatalyst for oxygen reduction and evolution reactions, *ACS Appl. Mater. Interfaces*, 2013, **5**, 5002–5008.

124 M. Sun, H. Liu, Y. Liu, J. Qu and J. Li, Graphene-based transition metal oxide nanocomposites for the oxygen reduction reaction, *Nanoscale*, 2015, **7**, 1250–1269.

125 Y. Liang, Y. Li, H. Wang, J. Zhou, J. Wang, T. Regier and H. Dai, Co(3)O(4) nanocrystals on graphene as a synergistic catalyst for oxygen reduction reaction, *Nat. Mater.*, 2011, **10**, 780–786.

126 Y. Liang, H. Wang, J. Zhou, Y. Li, J. Wang, T. Regier and H. Dai, Covalent hybrid of spinel manganese-cobalt oxide and graphene as advanced oxygen reduction electrocatalysts, *J. Am. Chem. Soc.*, 2012, **134**, 3517–3523.

127 J. Feng, Y. Liang, H. Wang, Y. Li, B. Zhang, J. Zhou, J. Wang, T. Regier and H. Dai, Engineering manganese oxide/nanocarbon hybrid materials for oxygen reduction electrocatalysis, *Nano Res.*, 2012, **5**, 718–725.

128 J.-S. Lee, T. Lee, H.-K. Song, J. Cho and B.-S. Kim, Ionic liquid modified graphene nanosheets anchoring manganese oxide nanoparticles as efficient electrocatalysts for Zn-air batteries, *Energy Environ. Sci.*, 2011, **4**, 4148.

129 J. Duan, S. Chen, S. Dai and S. Z. Qiao, Shape Control of Mn_3O_4 Nanoparticles on Nitrogen-Doped Graphene for Enhanced Oxygen Reduction Activity, *Adv. Funct. Mater.*, 2014, **24**, 2072–2078.

130 J. Zhang, C. Guo, L. Zhang and C. M. Li, Direct growth of flower-like manganese oxide on reduced graphene oxide towards efficient oxygen reduction reaction, *Chem. Commun.*, 2013, **49**, 6334–6336.

131 Z. S. Wu, S. Yang, Y. Sun, K. Parvez, X. Feng and K. Mullen, 3D nitrogen-doped graphene aerogel-supported Fe_3O_4 nanoparticles as efficient electrocatalysts for the oxygen reduction reaction, *J. Am. Chem. Soc.*, 2012, **134**, 9082–9085.

132 R. Zhou, Y. Zheng, D. Hulicova-Jurcakova and S. Z. Qiao, Enhanced electrochemical catalytic activity by copper

oxide grown on nitrogen-doped reduced graphene oxide, *J. Mater. Chem. A*, 2013, **1**, 13179.

133 L. Wang, A. Ambrosi and M. Pumera, "Metal-Free" Catalytic Oxygen Reduction Reaction on Heteroatom-Doped Graphene is Caused by Trace Metal Impurities, *Angew. Chem., Int. Ed.*, 2013, **52**, 13818–13821.

134 J. Masa, A. Zhao, W. Xia, Z. Sun, B. Mei, M. Muhler and W. Schuhmann, Trace metal residues promote the activity of supposedly metal-free nitrogen-modified carbon catalysts for the oxygen reduction reaction, *Electrochem. Commun.*, 2013, **34**, 113–116.

135 J. Masa, A. Zhao, W. Xia, M. Muhler and W. Schuhmann, Metal-free catalysts for oxygen reduction in alkaline electrolytes: influence of the presence of Co, Fe, Mn and Ni inclusions, *Electrochim. Acta*, 2014, **128**, 271–278.

136 H. T. Chung, J. H. Won and P. Zelenay, Active and stable carbon nanotube/nanoparticle composite electrocatalyst for oxygen reduction, *Nat. Commun.*, 2013, **4**, 1922.

137 L. Qu, Y. Liu, J.-B. Baek and L. Dai, Nitrogen-Doped Graphene as Efficient Metal-Free Electrocatalyst for Oxygen Reduction in Fuel Cells, *ACS Nano*, 2010, **4**, 1321–1326.

138 D. Geng, Y. Chen, Y. Chen, Y. Li, R. Li, X. Sun, S. Ye and S. Knights, High oxygen-reduction activity and durability of nitrogen-doped graphene, *Energy Environ. Sci.*, 2011, **4**, 760.

139 L. Lai, J. R. Potts, D. Zhan, L. Wang, C. K. Poh, C. Tang, H. Gong, Z. Shen, J. Lin and R. S. Ruoff, Exploration of the active center structure of nitrogen-doped graphene-based catalysts for oxygen reduction reaction, *Energy Environ. Sci.*, 2012, **5**, 7936.

140 M. Vikkisk, I. Kruusenberg, U. Joost, E. Shulga, I. Kink and K. Tammeveski, Electrocatalytic oxygen reduction on nitrogen-doped graphene in alkaline media, *Appl. Catal., B*, 2014, **147**, 369–376.

141 S. Yang, X. Feng, X. Wang and K. Mullen, Graphene-based carbon nitride nanosheets as efficient metal-free electrocatalysts for oxygen reduction reactions, *Angew. Chem., Int. Ed.*, 2011, **50**, 5339–5343.

142 Z. Lin, G. Waller, Y. Liu, M. Liu and C.-P. Wong, Facile Synthesis of Nitrogen-Doped Graphene *via* Pyrolysis of Graphene Oxide and Urea, and its Electrocatalytic Activity toward the Oxygen-Reduction Reaction, *Adv. Energy Mater.*, 2012, **2**, 884–888.

143 D. S. Su, J. Zhang, B. Frank, A. Thomas, X. Wang, J. Paraknowitsch and R. Schlögl, Metal-Free Heterogeneous Catalysis for Sustainable Chemistry, *ChemSusChem*, 2010, **3**, 169–180.

144 F. Pan, J. Jin, X. Fu, Q. Liu and J. Zhang, Advanced oxygen reduction electrocatalyst based on nitrogen-doped graphene derived from edible sugar and urea, *ACS Appl. Mater. Interfaces*, 2013, **5**, 11108–11114.

145 X. Li, H. Wang, J. T. Robinson, H. Sanchez, G. Diankov and H. Dai, Simultaneous Nitrogen Doping and Reduction of Graphene Oxide, *J. Am. Chem. Soc.*, 2009, **131**, 15939–15944.

146 L. Zhang and Z. Xia, Mechanisms of Oxygen Reduction Reaction on Nitrogen-Doped Graphene for Fuel Cells, *J. Phys. Chem. C*, 2011, **115**, 11170–11176.

147 X. Bo, C. Han, Y. Zhang and L. Guo, Confined nanospace synthesis of less aggregated and porous nitrogen-doped graphene as metal-free electrocatalysts for oxygen reduction reaction in alkaline solution, *ACS Appl. Mater. Interfaces*, 2014, **6**, 3023–3030.

148 B. Zheng, J. Wang, F.-B. Wang and X.-H. Xia, Synthesis of nitrogen doped graphene with high electrocatalytic activity toward oxygen reduction reaction, *Electrochem. Commun.*, 2013, **28**, 24–26.

149 H.-P. Cong, P. Wang, M. Gong and S.-H. Yu, Facile synthesis of mesoporous nitrogen-doped graphene: an efficient methanol–tolerant cathodic catalyst for oxygen reduction reaction, *Nano Energy*, 2014, **3**, 55–63.

150 Z. Lin, G. H. Waller, Y. Liu, M. Liu and C.-P. Wong, 3D Nitrogen-doped graphene prepared by pyrolysis of graphene oxide with polypyrrole for electrocatalysis of oxygen reduction reaction, *Nano Energy*, 2013, **2**, 241–248.

151 Y. Zhang, J. Ge, L. Wang, D. Wang, F. Ding, X. Tao and W. Chen, Manageable N-doped graphene for high performance oxygen reduction reaction, *Sci. Rep.*, 2013, **3**, 2771.

152 C. Zhang, R. Hao, H. Liao and Y. Hou, Synthesis of amino-functionalized graphene as metal-free catalyst and exploration of the roles of various nitrogen states in oxygen reduction reaction, *Nano Energy*, 2013, **2**, 88–97.

153 T. Xing, Y. Zheng, L. H. Li, B. C. C. Cowie, D. Gunzelmann, S. Z. Qiao, S. Huang and Y. Chen, Observation of Active Sites for Oxygen Reduction Reaction on Nitrogen-Doped Multilayer Graphene, *ACS Nano*, 2014, **8**, 6856–6862.

154 W. Ding, Z. Wei, S. Chen, X. Qi, T. Yang, J. Hu, D. Wang, L. J. Wan, S. F. Alvi and L. Li, Space-confinement-induced synthesis of pyridinic- and pyrrolic-nitrogen-doped graphene for the catalysis of oxygen reduction, *Angew. Chem., Int. Ed.*, 2013, **52**, 11755–11759.

155 Z. Luo, S. Lim, Z. Tian, J. Shang, L. Lai, B. MacDonald, C. Fu, Z. Shen, T. Yu and J. Lin, Pyridinic N doped graphene: synthesis, electronic structure, and electrocatalytic property, *J. Mater. Chem.*, 2011, **21**, 8038.

156 D. Higgins, Z. Chen, D. U. Lee and Z. Chen, Activated and nitrogen-doped exfoliated graphene as air electrodes for metal–air battery applications, *J. Mater. Chem. A*, 2013, **1**, 2639.

157 Y. Ito, H. J. Qiu, T. Fujita, Y. Tanabe, K. Tanigaki and M. Chen, Bicontinuous nanoporous N-doped graphene for the oxygen reduction reaction, *Adv. Mater.*, 2014, **26**, 4145–4150.

158 Z. Jiang, Z.-J. Jiang, X. Tian and W. Chen, Amine-functionalized holey graphene as a highly active metal-free catalyst for the oxygen reduction reaction, *J. Mater. Chem. A*, 2014, **2**, 441–450.

159 Y. Sun, C. Li and G. Shi, Nanoporous nitrogen doped carbon modified graphene as electrocatalyst for oxygen reduction reaction, *J. Mater. Chem.*, 2012, **22**, 12810.

160 W. Wei, H. Liang, K. Parvez, X. Zhuang, X. Feng and K. Mullen, Nitrogen-doped carbon nanosheets with size-defined mesopores as highly efficient metal-free catalyst for the oxygen reduction reaction, *Angew. Chem., Int. Ed.*, 2014, **53**, 1570–1574.

161 S. Yang, L. Zhi, K. Tang, X. Feng, J. Maier and K. Müllen, Efficient Synthesis of Heteroatom (N or S)-Doped Graphene Based on Ultrathin Graphene Oxide-Porous Silica Sheets for Oxygen Reduction Reactions, *Adv. Funct. Mater.*, 2012, **22**, 3634–3640.

162 E. Proietti, F. Jaouen, M. Lefèvre, N. Larouche, J. Tian, J. Herranz and J.-P. Dodelet, Iron-based cathode catalyst with enhanced power density in polymer electrolyte membrane fuel cells, *Nat. Commun.*, 2011, **2**, 416.

163 D. Zhao, J.-L. Shui, L. R. Grabstanowicz, C. Chen, S. M. Commet, T. Xu, J. Lu and D.-J. Liu, Highly Efficient Non-Precious Metal Electrocatalysts Prepared from One-Pot Synthesized Zeolitic Imidazolate Frameworks, *Adv. Mater.*, 2014, **26**, 1093–1097.

164 Y. Zhang, M. Chu, L. Yang, W. Deng, Y. Tan, M. Ma and Q. Xie, Synthesis and oxygen reduction properties of three-dimensional sulfur-doped graphene networks, *Chem. Commun.*, 2014, **50**, 6382–6385.

165 Y. Chen, J. Li, T. Mei, X. G. Hu, D. Liu, J. Wang, M. Hao, J. Li, J. Wang and X. Wang, Low-temperature and one-pot synthesis of sulfurized graphene nanosheets *viain situ* doping and their superior electrocatalytic activity for oxygen reduction reaction, *J. Mater. Chem. A*, 2014, **2**, 20714–20722.

166 I. Y. Jeon, H. J. Choi, S. M. Jung, J. M. Seo, M. J. Kim, L. Dai and J. B. Baek, Large-scale production of edge-selectively functionalized graphene nanoplatelets *via* ball milling and their use as metal-free electrocatalysts for oxygen reduction reaction, *J. Am. Chem. Soc.*, 2013, **135**, 1386–1393.

167 Z. Ma, S. Dou, A. Shen, L. Tao, L. Dai and S. Wang, Sulfur-doped graphene derived from cycled lithium-sulfur batteries as a metal-free electrocatalyst for the oxygen reduction reaction, *Angew. Chem., Int. Ed.*, 2015, **54**, 1888–1892.

168 M. Seredych and T. J. Bandosz, Confined space reduced graphite oxide doped with sulfur as metal-free oxygen reduction catalyst, *Carbon*, 2014, **66**, 227–233.

169 R. K. Shervedani and A. Amini, Carbon black/sulfur-doped graphene composite prepared by pyrolysis of graphene oxide with sodium polysulfide for oxygen reduction reaction, *Electrochim. Acta*, 2014, **142**, 51–60.

170 Z. Yang, Z. Yao, G. Li, G. Fang, H. Nie, Z. Liu, X. Zhou, X. A. Chen and S. Huang, Sulfur-Doped Graphene as an Efficient Metal-free Cathode Catalyst for Oxygen Reduction, *ACS Nano*, 2012, **6**, 205–211.

171 C. Zhang, N. Mahmood, H. Yin, F. Liu and Y. Hou, Synthesis of phosphorus-doped graphene and its multifunctional applications for oxygen reduction reaction and lithium ion batteries, *Adv. Mater.*, 2013, **25**, 4932–4937.

172 Y. Jiao, Y. Zheng, M. Jaroniec and S. Z. Qiao, Origin of the Electrocatalytic Oxygen Reduction Activity of Graphene-Based Catalysts: A Roadmap to Achieve the Best Performance, *J. Am. Chem. Soc.*, 2014, **136**, 4394–4403.

173 Z.-H. Sheng, H.-L. Gao, W.-J. Bao, F.-B. Wang and X.-H. Xia, Synthesis of boron doped graphene for oxygen reduction reaction in fuel cells, *J. Mater. Chem.*, 2012, **22**, 390–395.

174 Z. Yao, H. Nie, Z. Yang, X. Zhou, Z. Liu and S. Huang, Catalyst-free synthesis of iodine-doped graphene *via* a facile thermal annealing process and its use for electrocatalytic oxygen reduction in an alkaline medium, *Chem. Commun.*, 2012, **48**, 1027–1029.

175 D.-W. Wang and D. Su, Heterogeneous nanocarbon materials for oxygen reduction reaction, *Energy Environ. Sci.*, 2014, **7**, 576–591.

176 S. Bag, B. Mondal, A. K. Das and C. R. Raj, Nitrogen and Sulfur Dual-Doped Reduced Graphene Oxide: Synergistic Effect of Dopants Towards Oxygen Reduction Reaction, *Electrochim. Acta*, 2015, **163**, 16–23.

177 Y. Chang, F. Hong, C. He, Q. Zhang and J. Liu, Nitrogen and Sulfur Dual-Doped Non-Noble Catalyst Using Fluidic Acrylonitrile Telomer as Precursor for Efficient Oxygen Reduction, *Adv. Mater.*, 2013, **25**, 4794–4799.

178 C. H. Choi, M. W. Chung, H. C. Kwon, S. H. Park and S. I. Woo, B, N- and P, N-doped graphene as highly active catalysts for oxygen reduction reactions in acidic media, *J. Mater. Chem. A*, 2013, **1**, 3694.

179 Y. Zhao, L. Yang, S. Chen, X. Wang, Y. Ma, Q. Wu, Y. Jiang, W. Qian and Z. Hu, Can Boron and Nitrogen Co-doping Improve Oxygen Reduction Reaction Activity of Carbon Nanotubes?, *J. Am. Chem. Soc.*, 2013, **135**, 1201–1204.

180 S. Wang, E. Iyyamperumal, A. Roy, Y. Xue, D. Yu and L. Dai, Vertically Aligned BCN Nanotubes as Efficient Metal-Free Electrocatalysts for the Oxygen Reduction Reaction: A Synergetic Effect by Co-Doping with Boron and Nitrogen, *Angew. Chem., Int. Ed.*, 2011, **50**, 11756–11760.

181 S. Ding, S. Zheng, M. Xie, L. Peng, X. Guo and W. Ding, One-pot synthesis of boron-doped mesoporous carbon with boric acid as a multifunction reagent, *Microporous Mesoporous Mater.*, 2011, **142**, 609–613.

182 D. Golberg, Y. Bando, W. Han, K. Kurashima and T. Sato, Single-walled B-doped carbon, B/N-doped carbon and BN nanotubes synthesized from single-walled carbon nanotubes through a substitution reaction, *Chem. Phys. Lett.*, 1999, **308**, 337–342.

183 S. Wang, L. Zhang, Z. Xia, A. Roy, D. W. Chang, J. B. Baek and L. Dai, BCN graphene as efficient metal-free electrocatalyst for the oxygen reduction reaction, *Angew. Chem., Int. Ed.*, 2012, **51**, 4209–4212.

184 Y. Xue, D. Yu, L. Dai, R. Wang, D. Li, A. Roy, F. Lu, H. Chen, Y. Liu and J. Qu, Three-dimensional B,N-doped graphene foam as a metal-free catalyst for oxygen reduction reaction, *Phys. Chem. Chem. Phys.*, 2013, **15**, 12220–12226.

185 R. T. Paine and C. K. Narula, Synthetic routes to boron nitride, *Chem. Rev.*, 1990, **90**, 73–91.

186 Y. Zheng, Y. Jiao, L. Ge, M. Jaroniec and S. Z. Qiao, Two-Step Boron and Nitrogen Doping in Graphene for Enhanced Synergistic Catalysis, *Angew. Chem., Int. Ed.*, 2013, **125**, 3192–3198.

187 Y. Zheng, Y. Jiao, L. Ge, M. Jaroniec and S. Z. Qiao, Two-step boron and nitrogen doping in graphene for enhanced synergistic catalysis, *Angew. Chem., Int. Ed.*, 2013, **52**, 3110–3116.

188 J.-M. You, M. S. Ahmed, H. S. Han, J. E. Choe, Z. Üstündağ and S. Jeon, New approach of nitrogen and sulfur-doped

graphene synthesis using dipyrrolemethane and their electrocatalytic activity for oxygen reduction in alkaline media, *J. Power Sources*, 2015, **275**, 73–79.

189 X. Wang, J. Wang, D. Wang, S. Dou, Z. Ma, J. Wu, L. Tao, A. Shen, C. Ouyang, Q. Liu and S. Wang, One-pot synthesis of nitrogen and sulfur co-doped graphene as efficient metal-free electrocatalysts for the oxygen reduction reaction, *Chem. Commun.*, 2014, **50**, 4839–4842.

190 F. Razmjooei, K. P. Singh, M. Y. Song and J.-S. Yu, Enhanced electrocatalytic activity due to additional phosphorous doping in nitrogen and sulfur-doped graphene: a comprehensive study, *Carbon*, 2014, **78**, 257–267.

191 J. Liang, Y. Jiao, M. Jaroniec and S. Z. Qiao, Sulfur and nitrogen dual-doped mesoporous graphene electrocatalyst for oxygen reduction with synergistically enhanced performance, *Angew. Chem., Int. Ed.*, 2012, **51**, 11496–11500.

192 P. H. Matter, L. Zhang and U. S. Ozkan, The role of nanostructure in nitrogen-containing carbon catalysts for the oxygen reduction reaction, *J. Catal.*, 2006, **239**, 83–96.

193 Z. Chen, D. Higgins and Z. Chen, Electrocatalytic activity of nitrogen doped carbon nanotubes with different morphologies for oxygen reduction reaction, *Electrochim. Acta*, 2010, **55**, 4799–4804.

194 C. H. Choi, S. H. Park and S. I. Woo, Binary and Ternary Doping of Nitrogen, Boron, and Phosphorus into Carbon for Enhancing Electrochemical Oxygen Reduction Activity, *ACS Nano*, 2012, **6**, 7084–7091.

195 R. Li, Z. Wei and X. Gou, Nitrogen and Phosphorus Dual-Doped Graphene/Carbon Nanosheets as Bifunctional Electrocatalysts for Oxygen Reduction and Evolution, *ACS Catal.*, 2015, 4133–4142.

196 H. T. Chung, C. M. Johnston, K. Artyushkova, M. Ferrandon, D. J. Myers and P. Zelenay, Cyanamide-derived non-precious metal catalyst for oxygen reduction, *Electrochem. Commun.*, 2010, **12**, 1792–1795.

197 M. Ferrandon, A. J. Kropf, D. J. Myers, K. Artyushkova, U. Kramm, P. Bogdanoff, G. Wu, C. M. Johnston and P. Zelenay, Multitechnique Characterization of a Polyaniline–Iron–Carbon Oxygen Reduction Catalyst, *J. Phys. Chem. C*, 2012, **116**, 16001–16013.

198 Z. Mo, R. Zheng, H. Peng, H. Liang and S. Liao, Nitrogen-doped graphene prepared by a transfer doping approach for the oxygen reduction reaction application, *J. Power Sources*, 2014, **245**, 801–807.

199 D. Higgins, Z. Chen and Z. Chen, Nitrogen doped carbon nanotubes synthesized from aliphatic diamines for oxygen reduction reaction, *Electrochim. Acta*, 2011, **56**, 1570–1575.

200 Z. Chen, D. Higgins, H. Tao, R. S. Hsu and Z. Chen, Highly Active Nitrogen-Doped Carbon Nanotubes for Oxygen Reduction Reaction in Fuel Cell Applications, *J. Phys. Chem. C*, 2009, **113**, 21008–21013.

201 C. V. Rao, C. R. Cabrera and Y. Ishikawa, In Search of the Active Site in Nitrogen-Doped Carbon Nanotube Electrodes for the Oxygen Reduction Reaction, *J. Phys. Chem. Lett.*, 2010, **1**, 2622–2627.

202 J.-S. Lee, K. Jo, T. Lee, T. Yun, J. Cho and B.-S. Kim, Facile synthesis of hybrid graphene and carbon nanotubes as a metal-free electrocatalyst with active dual interfaces for efficient oxygen reduction reaction, *J. Mater. Chem. A*, 2013, **1**, 9603–9607.

203 D.-W. Wang, I. R. Gentle and G. Q. Lu, Enhanced electrochemical sensitivity of PtRh electrodes coated with nitrogen-doped graphene, *Electrochem. Commun.*, 2010, **12**, 1423–1427.

204 S. Park, Y. Hu, J. O. Hwang, E.-S. Lee, L. B. Casabianca, W. Cai, J. R. Potts, H.-W. Ha, S. Chen, J. Oh, S. O. Kim, Y.-H. Kim, Y. Ishii and R. S. Ruoff, Chemical structures of hydrazine-treated graphene oxide and generation of aromatic nitrogen doping, *Nat. Commun.*, 2012, **3**, 638.

205 P. Chen, T.-Y. Xiao, Y.-H. Qian, S.-S. Li and S.-H. Yu, A Nitrogen-Doped Graphene/Carbon Nanotube Nanocomposite with Synergistically Enhanced Electrochemical Activity, *Adv. Mater.*, 2013, **25**, 3192–3196.

206 S. Ratso, I. Kruusenberg, M. Vikkisk, U. Joost, E. Shulga, I. Kink, T. Kallio and K. Tammeveski, Highly active nitrogen-doped few-layer graphene/carbon nanotube composite electrocatalyst for oxygen reduction reaction in alkaline media, *Carbon*, 2014, **73**, 361–370.

207 Y. Ma, L. Sun, W. Huang, L. Zhang, J. Zhao, Q. Fan and W. Huang, Three-Dimensional Nitrogen-Doped Carbon Nanotubes/Graphene Structure Used as a Metal-Free Electrocatalyst for the Oxygen Reduction Reaction, *J. Phys. Chem. C*, 2011, **115**, 24592–24597.

208 H. W. Park, D. U. Lee, Y. Liu, J. Wu, L. F. Nazar and Z. Chen, Bi-Functional N-Doped CNT/Graphene Composite as Highly Active and Durable Electrocatalyst for Metal Air Battery Applications, *J. Electrochem. Soc.*, 2013, **160**, A2244–A2250.

209 D. C. Higgins, M. A. Hoque, F. Hassan, J.-Y. Choi, B. Kim and Z. Chen, Oxygen Reduction on Graphene–Carbon Nanotube Composites Doped Sequentially with Nitrogen and Sulfur, *ACS Catal.*, 2014, **4**, 2734–2740.

210 Z. Jin, H. Nie, Z. Yang, J. Zhang, Z. Liu, X. Xu and S. Huang, Metal-free selenium doped carbon nanotube/graphene networks as a synergistically improved cathode catalyst for oxygen reduction reaction, *Nanoscale*, 2012, **4**, 6455–6460.

211 H. Fei, R. Ye, G. Ye, Y. Gong, Z. Peng, X. Fan, E. L. G. Samuel, P. M. Ajayan and J. M. Tour, Boron- and Nitrogen-Doped Graphene Quantum Dots/Graphene Hybrid Nanoplatelets as Efficient Electrocatalysts for Oxygen Reduction, *ACS Nano*, 2014, **8**, 10837–10843.

